

This article should be cited as: Sharifzadeh M^{*}, Richard CJ, Liu K, Hellgardt K, Chadwick D, Shah N. (2015). An integrated process for biomass pyrolysis oil upgrading: the synergistic approach. *Biomass & Bioenergy*. 76, 108–117, ([Link](#)).

1 An Integrated Process for Biomass Pyrolysis Oil Upgrading: A Synergistic

2 Approach

3 M. Sharifzadeh^{a1}, C. Richard^b, K. Liu^b, K. Hellgardt^b, D. Chadwick^b and N. Shah^a

4

5 **Abstract-** Biomass pyrolysis is a promising path toward renewable liquid fuels. However, the calorific value of
6 the pyrolysis oil (PO), also known as bio-oil, is low due to the high content of organic oxygenates and water.
7 The oxygen content of PO can be reduced by hydrodeoxygenation, in which hydrogen is used to remove
8 oxygen. An economic disadvantage of hydrodeoxygenation pathway is its dependence on hydrogen as an
9 expensive feedstock. An alternative technology is to upgrade PO in hot, high pressure water, known as
10 hydrothermal processing. The present paper studies upgrading pyrolysis oil derived from Norwegian spruce by
11 (1) hydrodeoxygenation in a liquid hydrocarbon solvent using nanodispersed sulphide catalysts and (2)
12 hydrothermal treatment in near-supercritical water. Experimental results and simulation studies suggested
13 that if water soluble products are reformed for hydrogen production, the hydrodeoxygenation pathway would
14 be a net consumer of hydrogen, whilst the hydrothermal pathway could produce a significant hydrogen excess.
15 By comparison, the fuel yield from hydrodeoxygenation was significantly higher than hydrothermally treated
16 fuel. Therefore, in the present study, an integrated model was proposed which demonstrates that the
17 synergistic integration of hydrothermal and hydrodeoxygenation upgrading technologies can yield an optimal
18 configuration which maximises fuel production, whilst obviating the need to purchase hydrogen. In this
19 optimal configuration, 32% of raw pyrolysis-oil is hydrothermally treated and the rest is sent for
20 hydrodeoxygenation. The results of a techno-economic analysis suggests that if the proposed integrated
21 approach is used, it is possible to produce biofuel (43% gasoline, and 57% diesel) at a very competitive
22 minimum selling price of 428 \$ m⁻³ (1.62 \$/gallon).

23

24 **Key words:** Biomass fast pyrolysis, Pyrolysis oil upgrading, hydrodeoxygenation, hydrothermal treatment,
25 process integration, techno-economic analysis

¹ Corresponding Author: Dr Mahdi Sharifzadeh; Room C603, Roderic Hill Building, South Kensington Campus, Imperial College London, UK. SW7 2AZ. E-mail: mahdi@imperial.ac.uk; Tel: +44(0)7517853422

26 **1. Introduction**

27 The production of liquid fuels from biomass has the potential to diversify energy resources and
28 mitigate the environmental impacts associated with consumption of fossil-based energy resources.
29 Amongst various conversion pathways such as fermentation, hydrothermal liquefaction, pyrolysis,
30 and gasification [1], pyrolysis offers the cheapest route to renewable liquid fuels. Nonetheless, many
31 aspects of the pyrolysis pathway are still under investigation. The diverse array of research into
32 biomass pyrolysis is multi-disciplinary and multi-dimensional and includes Pyrolysis Oil (PO)
33 characterization [2-4], kinetic studies [5,6], computational fluid dynamics [7], design of new reactors
34 [8], microwave assisted pyrolysis [9-10], optimizing the PO yield [11], process intensification [12],
35 techno-economic analysis [13,14] environmental assessment [15], in addition to enterprise-wide and
36 supply chain optimization [16-18].

37 Despite various economic incentives, commercialization of biomass pyrolysis poses an important
38 challenge; the product of the pyrolysis reactions, called Pyrolysis Oil (PO), suffers from undesirable
39 properties. It has a high level of organic oxygenates which results in a low calorific value. PO is
40 highly acidic, and chemically unstable, which leads to polymerization and gradual increases in its
41 viscosity. In addition, due to the high water content (*ca.* 0.35 mass fraction) it is immiscible with
42 conventional fossil fuels. The technologies for the removal of oxygen and other heteroatoms in PO
43 are referred to as “upgrading”. Hydrodeoxygenation is the most common upgrading technology and
44 was originally inspired by hydrodesulfurization (HDS) and hydrodenitrogenation (HDN) from the
45 petroleum refining industry and coal liquefaction [19-23]. However, the amount of heteroatoms (i.e.,
46 oxygen) is an order of magnitude larger in the case of PO. The high oxygen content can lead to
47 excess coke formation [24]. As a resolution multistage hydrodeoxygenation has been proposed in
48 which first the PO is stabilized in a low temperature reactor and then a deeper hydrodeoxygenation
49 (HDO) is accomplished in the second-stage reactor at a higher temperature [25-27]. While
50 hydrodeoxygenation does not alter the boiling range of hydrocarbons significantly, cracking and

This article should be cited as: Sharifzadeh M*, Richard CJ, Liu K, Hellgardt K, Chadwick D, Shah N. (2015). An integrated process for biomass pyrolysis oil upgrading: the synergistic approach. *Biomass & Bioenergy*. 76, 108–117, ([Link](#)).

51 hydrocracking using zeolites are efficient methods to reduce the size of product molecules by
52 depolymerisation of heavy oligomers [28]. However, coking can be so severe that a fixed bed reactor
53 may become plugged quickly. Pretreatment using multistage HDO can mitigate the problem [29].
54 Recent research concerning catalysts for a low temperature first stage PO upgrading has tended
55 towards supported precious metals especially Ru or Pd with carbon as a support (e.g. [26], [30]). In
56 contrast, conventional refinery hydrotreating catalysts are based on Co-Mo or Ni-Mo sulphides
57 supported on alumina. These catalysts have found wide application in PO upgrading research [20-
58 23]. The use of a slurry reactor for a first stage catalytic hydrodeoxygenation has several attractions
59 [31]. It offers better temperature control which assists with control of coke formation, facilitates
60 catalyst withdrawal and replacement, and permits the use of microcatalysts. The present study of
61 pyrolysis oil upgrading is concerned with the use of unsupported mixed sulphide nanoparticle
62 catalysts. These are dispersed throughout the bulk of the pyrolysis oil/solvent liquid aiding the rapid
63 hydrogenation of free radicals, coke precursors, suppression of polymerisation etc. leading to
64 stabilisation of the oil. Nanoparticle catalysts also eliminate limitations which might arise from
65 internal mass transfer associated with the support pore structure. Unsupported nanosulphide
66 catalysts have been used in the hydrotreatment of heavy and residual oils [31], [32-34] and in coal
67 liquefaction [35]. Typically, the mass fractions of the catalysts were between 5×10^{-4} - 10^{-2} (500-
68 10,000ppm of metal) [32-33]. In the present work, Mo and Ni nanosulphides have been used in
69 combination as catalysts in the slurry phase for the first stage hydrodeoxygenation of the pyrolysis
70 oil. Mo and Ni nanosulphides were preferred due to the performance of Ni-Mo supported catalysts
71 for HDO (e.g. [36]). To our knowledge, this is the first time unsupported nanosulphide catalysts have
72 been used in the upgrading of pyrolysis oil (a recent patent application did not include any
73 experimental examples [37]).
74 An alternative process for the conversion of biomass to liquid fuels uses hot compressed water
75 (HCW) as a reaction medium. This “hydrothermal upgrading” technology dates back to pioneering
76 research in the 1970s to 1990s by Shell [38]. In hydrothermal upgrading (also known as aqueous-

This article should be cited as: Sharifzadeh M*, Richard CJ, Liu K, Hellgardt K, Chadwick D, Shah N. (2015). An integrated process for biomass pyrolysis oil upgrading: the synergistic approach. *Biomass & Bioenergy*. 76, 108–117, ([Link](#)).

77 phase processing) PO is mixed with a relatively large amount of water and processed at the near-
78 supercritical or supercritical phase. At 647.096 K and 217.755 MPa water becomes an
79 incompressible supercritical fluid [39]. Hot compressed water (HCW) or high temperature water
80 (HTW) are often used to describe both sub and supercritical water. Changes in the physical and
81 chemical properties of HCW become very apparent at around 300°C, at which the density and
82 polarity of HCW is similar to acetone, a polar organic solvent. This makes HCW a good solvent for the
83 solvation of non-polar organic compounds in PO, and provides a single phase medium for upgrading.
84 It is widely observed that at these conditions water exhibits distinct processing advantages such as
85 enhanced and tunable properties (e.g. solubility, solvent polarity, transport properties), and ease of
86 solvent removal [40]. Other advantages of this technology include avoiding phase change and
87 parasitic energy losses due to high-pressure processing, versatile chemistry to existing chemical and
88 fuel infrastructure, enhanced reaction rates [41], and minimal hydrogen consumption [42].
89 Hydrothermal processing can also be used to generate hydrogen and CO₂ as the co-product [43].
90 The combination of both hydrothermal and hydrodeoxygenation upgrading in an integrated process
91 is an attractive approach

92 The present paper proposes a novel integrated process for pyrolysis oil upgrading based on
93 synergies of hydrothermal and hydrodeoxygenation processes. In the proposed new process the
94 separated water soluble pyrolysis oil is used for hydrogen generation. A second stage
95 hydrodeoxygenation unit then follows where the water insoluble fraction is upgraded to biofuels.
96 While reforming the water soluble phase of bio-oil has been an active research area [44, 45], the
97 contribution of the present research is to propose an integrated configuration in which the
98 hydrothermal treatment can be considered both in parallel as well as in series to the
99 hydrodeoxygenation reactors to allow more flexibility. This configuration is also in contrast to
100 previous studies where an external source of hydrogen or a fraction of crude bio-oil was used for
101 hydrogen production. In the following, firstly, the experimental results for hydrodeoxygenation with
102 nanosulphide catalysts and hydrothermal processing without catalyst are presented. The

This article should be cited as: Sharifzadeh M*, Richard CJ, Liu K, Hellgardt K, Chadwick D, Shah N. (2015). An integrated process for biomass pyrolysis oil upgrading: the synergistic approach. *Biomass & Bioenergy*. 76, 108–117, ([Link](#)).

103 hydrodeoxygenation was done at conditions appropriate for a first stage slurry phase treatment
104 leading to aqueous phase separation with only a small extent of deoxygenation. Further
105 downstream deeper hydrodeoxygenation was included in the process scheme with details from ref
106 [46]. Based on the experimental results, preliminary studies were conducted in order to estimate
107 key process indicators (KPIs) for each technology in terms of mass and energy balances and
108 hydrogen requirements. Based on these preliminary studies, a new integrated upgrading process
109 was developed which exploits the advantages of both technologies in order to enhance process
110 profitability. A whole-process approach was applied in order to quantify the advantages of process
111 integration. The features of interest included process description, detailed economic analysis and
112 sensitivity analyses. It is shown that the novel integrated process where the water soluble phase is
113 applied for hydrogen production provides the most economic option for PO upgrading.

114 **2. Material and methods**

115 The following sections will discuss the experimental program regarding pyrolysis oil
116 hydrodeoxygenation and hydrothermal treatment. Another feature of interest is preliminary
117 evaluation of key process indicators, which enables proposition of an integrated process based on
118 the synergies of the studied upgrading technologies. This section also explains the modelling and
119 costing methods applied for techno economic analysis of the proposed process.

120 **2.1. Experimental studies**

121 The pyrolysis-oil studied was derived from Norwegian spruce, *Abis Picea*, supplied by Future Blends
122 Ltd. It contained aliphatic functionalities and phenolic residues, the latter being typically derived
123 from lignin, which is an important structural component in all woody biomass [47], Elemental
124 analysis and water content of the pyrolysis oil is given in Table 1. Analysis by quantitative ³¹P-NMR
125 [48] showed that hydroxyl groups comprised 58% of the organo-oxygen, of which aliphatic OH was
126 69% of the organo-OH.

127 Table 1 should be inserted here

This article should be cited as: Sharifzadeh M*, Richard CJ, Liu K, Hellgardt K, Chadwick D, Shah N. (2015). An integrated process for biomass pyrolysis oil upgrading: the synergistic approach. *Biomass & Bioenergy*. 76, 108–117, ([Link](#)).

128 The pyrolysis oil was subject to upgrading by hydrothermal treatment and hydrodeoxygenation. The
129 experimental details and a complete set of results are tabulated in the ESM.

130 **2.1.1. Hydrothermal upgrading (HTU)**

131 Hydrothermal upgrading was conducted in sealed stainless steel tubular batch reactors (8 cm³) at
132 380°C using a water to pyrolysis oil ratio of 3. The hydrothermal upgrading was carried out in the
133 absence of catalysts. A reduced density of 1.0 was chosen for the upgrading because it is well above
134 $\rho_r = 0.3$ which was reported to be the minimum value at which a model oil would be soluble in HCW
135 [49]. (Reduced density was estimated by the equation: $\rho_r = \rho_w/\rho_{w,c}$; (ρ_w = mass of water/reactor
136 volume), where $\rho_{w,c} = 375 \text{ kg m}^{-3}$ is the value of pure supercritical water [10]. The reaction
137 temperature of 380°C was used because this was the temperature at which the CH₃O- bond in
138 guaiacol was reported to hydrolyse to give catechol and methanol [50]. The dielectric constant at
139 the autogenic pressures generated by HCW at 380°C, would be sufficient to stabilise any reaction
140 intermediates formed in ionic reactions [39], [49]. Additionally, the ionic product of HCW increases
141 threefold from $10^{-13.99}$ to $10^{-11.30}$ in the direction of 25 to 300°C [39], [49]; this means that near
142 supercritical HCW can enhance the cleavage of C-O bonds by acid and base catalysed reactions [51].
143 The products from hydrothermal upgrading the pyrolysis oil were phase-separated. The water
144 soluble pyrolysis oil (WSPO) was easily separated. The water insoluble PO was dissolved in acetone
145 for characterization. Elemental analysis of the water insoluble PO is given in Table 2. The reduction
146 of the oxygen content compared to the original pyrolysis oil means that less hydrogen is needed for
147 the second-stage hydrodeoxygenation.

148 Table 2 should be inserted here

149 Gas yields were very low, especially at short residence times (Table S2 in ESM). Hydrogen can react
150 with oxygen to give water, and insoluble hydrocarbons. However the absence of catalyst and a
151 relatively mild reaction temperature of 380°C did not give sufficient hydrogen production, to
152 remove the oxygenates in HCW [51-53].

This article should be cited as: Sharifzadeh M*, Richard CJ, Liu K, Hellgardt K, Chadwick D, Shah N. (2015). An integrated process for biomass pyrolysis oil upgrading: the synergistic approach. *Biomass & Bioenergy*. 76, 108–117, ([Link](#)).

153 Total organic carbon (TOC) analysis of the separated water from the upgraded pyrolysis oil, showed
154 that when the reactor is cooled immediately after reaching 380°C, about 40% of the carbon in the
155 original PO will be associated with components which are water soluble (Table S3 in ESM). The
156 nature of water soluble organic oxygenates were determined by GC-MS (Table S6 in ESM). The high
157 solubility of these components was due to hydrophilic alcoholic OH, carbonyl C=O and acidic COOH
158 functionalities. This percentage of these functionalities was observed to decrease with residence
159 time as they were converted to water insoluble pyrolysis oil (WIPO), char, and light gases (Table S2 in
160 ESM). The results suggest that short residence time hydrothermal upgrading is an efficient method
161 to extract oxygenated components from the carbon rich water insoluble phase.

162 **2.1.2. Hydrodeoxygenation (HDO)**

163 The hydrodeoxygenation of pyrolysis oil carried out in a Parr 100 cm³ stainless steel autoclave with
164 purpose-made glass liner at 250°C and a hydrogen pressure (cold) of 5 MPa. Dodecane was used as
165 solvent in a constant oil/solvent weight ratio = 0.5. Sulphur with a mass fraction of 10⁻⁴ (100 ppm)
166 was added to the reaction mixture using dibutyl disulphide as a precursor. Under the reaction
167 conditions dibutyl disulphide is expected to be rapidly converted to H₂S.

168 Mo and Ni nanosulphide catalysts were produced in situ in the autoclave at 300°C using metal
169 precursor compounds dissolved in the hydrocarbon solvent containing the required amount of
170 dibutyl disulphide. Mo naphthenate and Ni naphthenate were used as the precursors to give mass
171 fractions of 2×10⁻³ (2000ppm) Mo and 4.9×10⁻³ (490ppm) Ni in the final hydrodeoxygenation
172 reaction mixture corresponding to a Ni/Mo mole ratio of 0.4. Under these conditions the resulting
173 MoS₂ catalyst particles were determined by previous TEM studies to be typically 8nm in size with
174 limited stacking of 3 to 4 layers. The released H₂S was purged from the autoclave by N₂ prior to
175 addition of the pyrolysis oil and remainder of the solvent.

176 The hydro-deoxygenated pyrolysis oil separated easily into a water soluble phase and a water
177 insoluble (oil/solvent) phase. The amount of residue or coke formation was small. Gas yields were

This article should be cited as: Sharifzadeh M*, Richard CJ, Liu K, Hellgardt K, Chadwick D, Shah N. (2015). An integrated process for biomass pyrolysis oil upgrading: the synergistic approach. *Biomass & Bioenergy*. 76, 108–117, ([Link](#)).

178 also small. The results of upgrading are summarised in Table 3. The compounds present in the water
179 soluble phase and the water insoluble phase were analysed by GC-MS (Table S8 ESM).

180 Table 3 should be inserted here

181 The high concentration of carbon in the recovered water soluble phase suggests that a significant
182 fraction of organo-OH compounds dissolve in the water rather than undergo HDO. The organo-
183 compounds present in the water soluble phase were analysed by GC-MS. The most significant
184 compounds were acids, mainly acetic with some C4 and C5 acids (Table S7, ESM). This suggests that
185 at the reaction conditions there is some degree of parallel hydrothermal treatment possibly
186 catalysed by the nanosulphide catalysts or derivatives thereof. ICP analysis of the recovered water
187 soluble phase (ESM) did not detect any significant amount of Ni or Mo. It is assumed therefore that
188 the catalysts remain associated with the residue

189 **2.2. Process design and economic evaluation**

190 The major part of the research involved process modelling and economic analysis. Firstly, the key
191 indicators of hydrothermal upgrading and hydrodeoxygenation processes were identified using
192 simplified process modelling. These preliminary studies enabled proposition of an integrated process
193 with enhanced economic performance, and was modelled and studied in detail. Finally, the paper
194 concludes with the results and discussions.

195 **2.2.1. Preliminary process modelling and evaluation**

196 The aforementioned experimental results were firstly applied for preliminary process modelling. The
197 simplified process flow diagrams are shown in Figs. 1a and 1b, and discussed below.

198 Fig. 1 should be inserted here.

199 In the hydrodeoxygenation process, the solvent were mixed with the nano-catalysts precursors and
200 sulphiding agent (Mo-Naph, Ni-Napt, DDS) in the solvent preparation vessel. Only an n-hydrocarbon,
201 n-dodecane, was considered as solvent. H-donor solvents such as tetralin, did not result in significant
202 improvement in the product yields and offer little advantage for the dispersed nanocatalysts, and is

203 significantly more expensive than n-hydrocarbons. The catalyst-carrying solvent is then mixed with
204 the PO at the mass ratio of 2.14:1. Hydrogen was directly injected to the slurry reactor. By
205 comparison, in the hydrothermal upgrading, the PO is mixed with the water at the mass ratio of
206 1:2.98 and fed to the reactor at temperature of 380°C. The autogenic pressure was not measured
207 directly but was estimated to be 22 MPa. The choice of solvent ratios was based on earlier studies in
208 hydrothermal processing [48]. No catalyst was used in the hydrothermal upgrading studies.

209 In both upgrading processes, the effluents of the first-stage upgrading process are phase-separated.
210 The water insoluble pyrolysis oil (WIPO) is sent to the second-stage hydrodeoxygenation, while the
211 water soluble pyrolysis oil (WSPO) is sent to the reformers for hydrogen production. These simplified
212 models enable calculating several important key process indicators, shown in Table 4. These
213 indicators suggest that the hydrodeoxygenation process features the highest fuel yield of 65.2%.
214 However, this process suffers from a hydrogen deficit and produces only 40% of its hydrogen
215 requirements. By comparison, the process with first-stage hydrothermal upgrading does not
216 produce significant fuel but features a large hydrogen surplus. These observations suggest that by
217 integrating the two hydrothermal and hydrodeoxygenation technologies, it is possible to design a
218 process which is self-sufficient and does not require any external source of hydrogen. The new
219 process is shown in Fig. 2. The crude PO is split between the two first-stage reactors. 31.85% of the
220 initial crude PO is sent to the hydrothermal upgrading reactor and the rest was processed in the
221 hydro-treatment reactors. The split ratio (i.e., 0.3185) was optimized so the hydrogen production
222 meets the hydrodeoxygenation requirements and the overall process is self-sustained. The effluents
223 of both reactors are cooled and phase separated. The water insoluble pyrolysis oil in addition to the
224 solvent are sent to the second-stage hydrodeoxygenation reactor. The water soluble pyrolysis oil is
225 sent for hydrogen production to Section 500 of the process.

226 Table 4 should be inserted here

227 Fig. 2 should be inserted here.

228

229 **2.2.2. Detailed process modelling**

230 Fig. 3 shows the overall process block diagram. The biomass is first fed into the Pyrolysis Section
231 (100), where it is converted to PO. The PO is then sent to the Upgrading Section (200). As discussed
232 earlier, the upgrading section exploits two parallel first-stage reactors and will benefit from the
233 desirable aspects of hydrothermal upgrading as well as hydrodeoxygenation technologies. The water
234 insoluble PO is later upgraded in the second-stage hydrodeoxygenation reactor for complete
235 hydrodeoxygenation. The upgraded PO is sent to Separation Section (300) where it is resolved to
236 gasoline and diesel products. In addition, the solvent is separated and recycled to the upgrading
237 section. Furthermore, Section 300 is integrated to a hydrocracking reactor (Section 400), where
238 heavy-ends are cracked into lighter higher-value products. The water soluble pyrolysis oil (WSPO)
239 from Upgrading Section (200) is fed to the Hydrogen Production Section (500), which supplies the
240 hydrogen required by hydro-treatment and hydrocracking reactors. All the sub-processes (100-500)
241 were modelled in detail. The process descriptions and applied modelling techniques are reported in
242 the Electronic Supplementary Material (ESM). The results of detailed process models were applied
243 for calculating the operating costs and purchased equipment costs, needed for the economic
244 analysis, as discussed later.

245 Fig. 3 should be inserted here.

246 **2.3. Economic evaluation**

247 The process throughput was considered to be 2000 ton per day of biomass on a dry basis, similar to
248 a previous study by DOE [46]. In order to evaluate the economic performance of the new process,
249 minimum fuel selling price (MFSP) was calculated, and compared to the benchmarks from literature
250 [46]. In order to calculate the MFSP, the net present value of the project was calculated. The
251 operating costs were evaluated based on the mass and energy balances from process simulator. In
252 addition, the purchased and installed equipment costs of conventional unit operations were

This article should be cited as: Sharifzadeh M*, Richard CJ, Liu K, Hellgardt K, Chadwick D, Shah N. (2015). An integrated process for biomass pyrolysis oil upgrading: the synergistic approach. *Biomass & Bioenergy*. 76, 108–117, ([Link](#)).

253 evaluated using Aspen Economic Analyzer™. However for the case of nonconventional equipment
254 such as reformers, the costs were calculated with respect to data from the literature [46]:

$$255 \quad \text{New cost} = \text{Base cost} * \left(\frac{\text{New size}}{\text{Base size}} \right)^{f_{\text{scale}}} \quad (1)$$

256 Given the total purchased equipment costs (TPEC), the total indirect costs (TIC) can be estimated by
257 summing the value of the engineering costs (32% of TPEC), construction costs (34% of TPEC), legal
258 and contractors fees (23% of TPEC) and project contingency (37% of TPEC). The fixed capital
259 investment (FCI) is the sum of Total Direct Installed Costs (TDC) and TIC. The total capital costs
260 include FCI and land cost (6% of TPEC) and the working capital (5% FCI) [46]. The variable operating
261 costs including raw materials, utilities, and waste disposal charges are summarized in Table 5. The
262 fixed operating costs including labour, overheads (95% of labour cost), maintenance (4% of TCI), and
263 insurance (4% of TCI) are scaled up based on Philipp, *et al.*'s study [55]. In the absence of economic
264 data, it was assumed that the new catalyst costs 7% of the final fuel product. This is a conservative
265 assumption because firstly, the hydrothermal reactor does not require any catalyst. Secondly, the
266 hydrodeoxygenation catalyst is a dispersed nanoparticle type which does not require a catalyst
267 support. Furthermore, due to the enhanced transport and heat transfer properties significantly less
268 catalyst is needed.

269

Table 5 should be inserted here

270 The NPVs were calculated using a discounted cash flow method (10% discount rate) for a period of
271 20 years, which is the assumed plant lifetime. The plant was assumed to be 100% equity with 2.5
272 years as a construction period and 6 months as the start-up time. All costs in this study were indexed
273 to the reference year of 2012. The MPSPs refers the product price at which the net present value of
274 the project is zero at a set discounted rate of 10%. The fuel price is defined as the weighted average
275 of gasoline (42.8%) and diesel (57.2%) prices. The price of petroleum-derived fuel [58] was used to
276 adjust all other fuel prices from literature to the reference year of 2012.

277 **3. Results and discussions**

278 The following sections present and discuss the results of the technoeconomic analysis of the
279 proposed process. The features of interest are minimum fuel selling price and its
280 comparison with competitive scenarios and sensitivity analysis of the results with respect to
281 underlying modelling and economic assumptions.

282 **3.1. Minimum Fuel selling Prices (MFSP)**

283 Fig. 4 shows the results of the economic analysis. The minimum fuel selling price (MFSP) is compared
284 with three benchmark prices from the literature. They are fuel price when hydrogen is produced
285 from reforming natural gas [46], fuel price when the bio-process is integrated to a conventional
286 refinery [46], and the price of petroleum-derived fuel [58]. While comparison with petroleum-
287 derived fuels is illustrative for potential commercialization of the proposed technology, such
288 comparison is subject to uncertainties in the volatile energy market. Fig 4 shows that the MFSP of
289 $428 \text{ \$ m}^{-3}$ (equivalent to 1.62 $\text{\$/Gallon}$) in the proposed process outperforms all these benchmarks.
290 The reason is that in the proposed process, by optimizing ratio between the two upgrading
291 technologies (i.e., HDO & HTU), the yield of final fuel is maximized, the hydrogen consumption is
292 minimized and only low quality materials are used for hydrogen production.

293 In order to evaluate the robustness the calculated MFSP with respect to the important model
294 parameters, a set of sensitivity analyses were conducted. Figs. 5 and 6 report the result of these
295 analyses. Fig 5 shows the sensitivity of the MFSP with respect to working capital, 1st stage HTU yield,
296 catalysts price, income tax, 1st stage HDO, the fraction of pyrolysis oil needed to be processed in HTU
297 (which represents the overall hydrogen requirement), and biomass price. In the present research, an
298 equilibrium yield of hydrogen was assumed. However, coke formation is reported to reduce the
299 hydrogen yield and catalyst life depending on the steam-to-carbon ratio, catalyst, and temperature
300 [59, 60]. The sensitivity of the minimum fuel selling price to this assumption is analysed based on the
301 fraction of pyrolysis oil sent to hydrothermal upgrading reactor (R-202). The implication is that if the

This article should be cited as: Sharifzadeh M*, Richard CJ, Liu K, Hellgardt K, Chadwick D, Shah N. (2015). An integrated process for biomass pyrolysis oil upgrading: the synergistic approach. *Biomass & Bioenergy*. 76, 108–117, ([Link](#)).

302 actual yield of hydrogen production is less than the calculated values, more pyrolysis oil must be
303 sent to the hydrothermal upgrading (HTU) reactor. Clearly, there remains a need for further research
304 to find stable, efficient catalysts for the steam reforming unit.

305 Fig. 6 shows the effect of process scale (represented by processed biomass-tpd) on the MFSP. This
306 figure suggests that for small-scale plants (< 500 tpd), the produced biofuel may not be economically
307 competitive anymore.

308 Fig. 4 should be inserted here.

309 Fig. 5 should be inserted here.

310 Fig. 6 should be inserted here.

311 **3.2. Total direct installed cost and operating costs**

312 Figs. 7 and 8 report the direct installed costs and utility costs, in addition to the contribution of each
313 sub-process to these costs. Fig. 7 reports that the total amount of direct installed costs is 240.3
314 MM\$, from which 45% was associated with hydrogen production section (500). This is because
315 WSBO is relatively dilute resulting in larger process equipment. The second largest contribution is
316 made by biomass pyrolysis section (100). This observation is consistent with other benchmarks *e.g.*,
317 [46].

318 Fig. 8 reports the contribution of each sub-process to the utility costs. The largest contributors to
319 electricity costs are the Upgrading (200) and Hydrogen Production (500) Sections. The Hydrogen
320 Production Section requires electricity for compression of the combustion air and operating the air-
321 cooler; Upgrading Section consumes electricity for pumping the reactor feeds and operating the air-
322 cooler. Steam is consumed in Separation Section (300) to provide heating duties in the distillation
323 columns, but it is also produced in Hydrogen Production Section (500) through heat recovery from
324 hot gases. The heating duties of reactors in Upgrading Section were supplied by the fire-heaters. The
325 costs of cooling water were moderate and were distributed between Pyrolysis, Upgrading and
326 Separation Sections.

This article should be cited as: Sharifzadeh M^a, Richard CJ, Liu K, Hellgardt K, Chadwick D, Shah N. (2015). An integrated process for biomass pyrolysis oil upgrading: the synergistic approach. *Biomass & Bioenergy*. 76, 108–117, ([Link](#)).

327 Fig. 7 should be inserted here.

328 Fig. 8 should be inserted here.

329 **4. Conclusions**

330 The present research studied hydrothermal upgrading and hydro-treatment of biomass pyrolysis oil.
331 The experimental results showed very different characteristics for these two technologies. While
332 pyrolysis oil hydrodeoxygenation gives high fuel yield, it suffers from hydrogen deficit, i.e., the
333 amount of produced hydrogen from reforming the water soluble pyrolysis oil (WSPO) is insufficient
334 for hydrodeoxygenation of the rest of pyrolysis oil (PO). By comparison, the fuel yield of PO
335 hydrothermal upgrading is not significant but it has the potential for producing large amounts of
336 hydrogen. These observations suggested that an integrated configuration utilizing the two
337 technologies can produce the maximum fuel and would be self-sufficient with respect to the
338 hydrogen requirement. It was shown that the proposed integrated process for PO upgrading offers
339 several advantages: the fuel production is maximized using PO hydrodeoxygenation and hydrogen
340 production is maximized using hydrothermal upgrading. In addition, the latter process does not
341 require hydrogen which results in reduced hydrogen requirements. The present research also
342 studied the economic implication of the new process. It was shown that the optimized configuration
343 is able to reduce the costs significantly and produce the fuel at a minimum price of 428 \$ m⁻³. The
344 upgrading section was found to be the largest contributor to the operating costs. In addition, due to
345 diluted water-soluble pyrolysis oil, hydrogen production required the largest capital investment.
346 Finally, the results of sensitivity analyses suggested that the process economy is robust to changes in
347 the modelling parameters, and the target minimum fuel selling price is achievable.

348 **Notes**

349 ^a Centre for Process Systems Engineering (CPSE), Department of Chemical Engineering, Imperial
350 College London, South Kensington, London SW7 2AZ, UK.

This article should be cited as: Sharifzadeh M*, Richard CJ, Liu K, Hellgardt K, Chadwick D, Shah N. (2015). An integrated process for biomass pyrolysis oil upgrading: the synergistic approach. *Biomass & Bioenergy*. 76, 108–117, ([Link](#)).

351 ^b Department of Chemical Engineering, Imperial College London, South Kensington, London
352 SW7 2AZ, UK.

353 **Acknowledgements**

354 The financial support of the Carbon Trust under the “Pyrolysis Challenge” is gratefully
355 acknowledged. We thank Future Blends Ltd. for supplying the pyrolysis oil. We are grateful to Dr
356 John Halket of Specialist Bioanalytical Services for assistance with GC-MS analysis, Mr Bavish
357 Patel for assistance with hydrothermal experiments. This work is dedicated to the late David
358 Penfold who was instrumental in setting up the Pyrolysis Challenge research programme under
359 which this work was funded.

360 **References**

361 **References**

- 362 [1] Naik SN, Goud VV, Rout PK, Dalai AK. Production of first and second generation biofuels: A
363 comprehensive review. *Renew Sust Energ Rev*, 2010; 14 (2): 578-97.
- 364 [2] Azeez AM, Meier D, Odermatt J, Willner T. Fast Pyrolysis of African and European
365 Lignocellulosic Biomasses Using Py-GC/MS and Fluidized Bed Reactor. *Energy Fuel*, 2010; 24
366 (3): 2078–85.
- 367 [3] Ben H, Ragauskas AJ. NMR Characterization of Pyrolysis Oils from Kraft Lignin. *Energy Fuel*,
368 2011; 25 (5): 2322–32.
- 369 [4] Ben H, Ragauskas AJ. Comparison for the compositions of fast and slow pyrolysis oils by NMR
370 Characterization. *Bioresourc Technol*, 2013 Nov; 147: 577–84.
- 371 [5] Mettler MS, Vlachos DG, Dauenhauer PJ. Top ten fundamental challenges of biomass
372 pyrolysis for biofuels. *Energy Environ Sci*, 2012; 5 (7): 7797-809.
- 373 [6] White JE, Catallo WJ, Legendre BL. Biomass pyrolysis kinetics: A comparative critical review
374 with relevant agricultural residue case studies. *J Anal Appl Pyrol*, 2011; 91 (1): 1–33.
- 375 [7] Papadakis K, Gu S, Bridgwater AV, Gerhauser H. Application of CFD to model fast pyrolysis of

This article should be cited as: Sharifzadeh M*, Richard CJ, Liu K, Hellgardt K, Chadwick D, Shah N. (2015). An integrated process for biomass pyrolysis oil upgrading: the synergistic approach. *Biomass & Bioenergy*. 76, 108–117, ([Link](#)).

- 376 biomass. *Fuel Process Technol*, 2009; 90 (4): 504–12.
- 377 [8] Isahak WNRW, Hisham MWM, Yarmo MA, Hin TY. A review on bio-oil production from
378 biomass by using pyrolysis method. *Renew Sust Energ Rev*, 2012; 16 (8): 5910–23.
- 379 [9] Motasemi F, Afzal MT. A review on the microwave-assisted pyrolysis technique. *Renew Sust*
380 *Energ Rev*, 2013 Dec; 28: 317–30.
- 381 [10] Borges FC, Du Z, Xie Q, Trierweiler JO, Cheng Y, Wan Y, et al. Fast microwave assisted
382 pyrolysis of biomass using microwave Absorbent. *Bioresourc Technol*, 2014 Mar; 156: 267-4.
- 383 [11] Akhtar J, Amin NS. A review on operating parameters for optimum liquid oil yield in
384 biomass pyrolysis. *Renew Sust Energ Rev*, 2012; 16 (7): 5101–9.
- 385 [12] Sadhukhan J. Multiscale simulation for high efficiency biodiesel process intensification. In:
386 Bogle IDL, Fairweather M (Editors), *Computer Aided Chemical Engineering, Proceedings of*
387 *the 22nd European Symposium on Computer Aided Process Engineering*, 17-20 June 2012,
388 London, 30: 1023-7.
- 389 [13] Brown T R, Thilakaratne R, Brown R C, Hu G. Techno-economic analysis of biomass to
390 transportation fuels and electricity via fast pyrolysis and hydroprocessing. *Fuel*, 2013 Apr;
391 106: 463–9.
- 392 [14] Wright MM, Daugaard DE, Satrio JA, Brown RC. Techno-economic analysis of biomass fast
393 pyrolysis to transportation fuels. *Fuel*, 2010; 89 (1): S2–S10.
- 394 [15] Gebreslassie BH, Slivinsky M, Wang B, You F. Life cycle optimization for sustainable design
395 and operations of hydrocarbon biorefinery via fast pyrolysis, hydrotreating and
396 hydrocracking. *Comput Chem Eng*, 2013 Mar; 50: 71– 91.
- 397 [16] Kim J, Realff M J, Lee J H, Whittaker C, Furtner L. Design of biomass processing network for
398 biofuel production using an MILP model. *Biomass Bioenerg*, 2011; 35 (2): 853-71
- 399 [17] Akgul O, Shah N, Papageorgiou L G. Economic optimisation of a UK advanced biofuel supply
400 chain Economic optimisation of a UK advanced biofuel supply chain. *Biomass Bioenerg*, 2012
401 June; 41: 57–72.

This article should be cited as: Sharifzadeh M*, Richard CJ, Liu K, Hellgardt K, Chadwick D, Shah N. (2015). An integrated process for biomass pyrolysis oil upgrading: the synergistic approach. *Biomass & Bioenergy*. 76, 108–117, ([Link](#)).

- 402 [18] Braimakisa K, Atsoniosa K, Panopoulos KD, Karellas S, Kakaras E. Economic evaluation of
403 decentralized pyrolysis for the production of bio-oil as an energy carrier for improved
404 logistics towards a large centralized gasification plant. *Renew Sust Energ Rev*, 2014 July; 35:
405 57–72.
- 406 [19] Elliott DC. Historical Developments in Hydroprocessing Bio-oils. *Energ Fuels*, 2007; 21 (3):
407 1792-815
- 408 [20] Huber GW, Iborra S, Corma A. Synthesis of transportation fuels from biomass: chemistry,
409 catalysts, and engineering. *Chem Rev*, 2006; 106 (9): 4044-98
- 410 [21] Mortensen PM, Grunwaldt J-D, Jensen PA, Knudsen KG, Jensen AD. A review of catalytic
411 upgrading of bio-oil to engine fuels. *Appl Catal A-Gen*, 2011; 407(1-2): 1-19
- 412 [22] Saidi M, Samimi F, Karimipourfard D, Nimmanwudipong T, Gates BC, Rahimpour MR.
413 Upgrading of lignin-derived bio-oils by catalytic hydrodeoxygenation. *Energ Environ Sci*,
414 2014; 7 (1); 103–29.
- 415 [23] de Miguel Mercader F, Groeneveld MJ, Kersten SRA, Geantet C, Toussaint G, Way NWJ, et
416 al. Hydrodeoxygenation of pyrolysis oil fractions: process understanding and quality
417 assessment through co-processing in refinery units. *Energ Environ Sci*, 2011; 4 (3): 985-97.
- 418 [24] Zacher AH, Olarte MV, Santosa DM, Elliott DC, Jones SB. A review and perspective of recent
419 bio-oil hydrotreating research. *Green Chem.*, 2014; 16 (2): 491-515.
- 420 [25] Baker EG, Elliott DC. Catalytic upgrading of biomass pyrolysis oils. In: Soltes EJ, Milne TA,
421 editors. *Pyrolysis oils from biomass*, American Chemical Society, Washington, DC. 1988, p.
422 883–95.
- 423 [26] Vispute TP, Zhang H, Sanna A, Xiao R, Huber GW. Renewable Chemical Commodity
424 Feedstocks from Integrated Catalytic Processing of Pyrolysis Oils. *Science*, 2010; 330 (6008):
425 1222-7.

This article should be cited as: Sharifzadeh M*, Richard CJ, Liu K, Hellgardt K, Chadwick D, Shah N. (2015). An integrated process for biomass pyrolysis oil upgrading: the synergistic approach. *Biomass & Bioenergy*. 76, 108–117, ([Link](#)).

- 426 [27] McCall MJ, Brandvold TA, Elliott DC, inventors; Uop Llc., assignee. Fuel and fuel blending
427 components from biomass derived pyrolysis oil. United States patent US 8329969 B2. 2012
428 Dec 11.
- 429 [28] Xiu S, Shahbazi A. Bio-oil production and upgrading research: A review. *Renew Sust Energ*
430 *Rev*, 2012, 16 (7), 4406–14.
- 431 [29] Taarning E, Osmundsen CM, Yang X, Voss B, Andersen SI, Christensen CH. Zeolite-catalyzed
432 biomass conversion to fuels and chemicals. *Energ Environ Sci*, 2011; 4 (3): 793–804.
- 433 [30] Elliot DC, Hu J, Hart TR, Neuenschwander GG, inventors; Battelle Memorial Institute,
434 assignee. Reacting the bio-oil and hydrogen over palladium catalyst, heating; producing a
435 liquid oil from the reaction of the bio-oil and hydrogen; bioethanol. United States patent
436 US7425657 B1. 2008 Sep 16.
- 437 [31] Bauer L, McCall M, Boldingh E, inventors; Uop Llc., assignee. Slurry Hydroconversion of
438 Biorenewable Feedstocks. United States Patent US8022259 B2. 2011 Sep 20.
- 439 [32] Panariti N, Del Bianco A, Del Piero G, Marchionna M. Petroleum residue upgrading with
440 dispersed catalysts: Part 1. Catalysts activity and selectivity. *Appl Catal A-Gen*, 2000; 204 (2):
441 203-13.
- 442 [33] Bellussi, G, Rispoli, G, Landoni, A, Millini, R, Molinari, D, Montanari, E, Moscotti, D, Pollesel,
443 P. Hydroconversion of heavy residues in slurry reactors: developments and perspectives. *J*
444 *Catal*, 2013 Dec; 308: 189-200.
- 445 [34] Fixari B, Peureux S, Elmouchnino J, Le Perchec P, Vrinat M, Morel F. New Developments in
446 Deep Hydroconversion of Heavy Oil Residues with Dispersed Catalysts. 1. Effect of Metals
447 and Experimental Conditions. *Energ Fuel*, 1994; 8 (3): 588-92.
- 448 [35] Curtis CW, Cassell FN. Investigation of the role of hydrogen donation in thermal and
449 catalytic coprocessing. *Energ Fuel*, 1988; 2 (1): 1 -8.
- 450 [36] He Z, Wang X. Hydrodeoxygenation of model compounds and catalytic systems for
451 pyrolysis bio-oils upgrading. *Catal Sustainable Energy*, 2012 Oct; 1: 28–52.

This article should be cited as: Sharifzadeh M*, Richard CJ, Liu K, Hellgardt K, Chadwick D, Shah N. (2015). An integrated process for biomass pyrolysis oil upgrading: the synergistic approach. *Biomass & Bioenergy*. 76, 108–117, ([Link](#)).

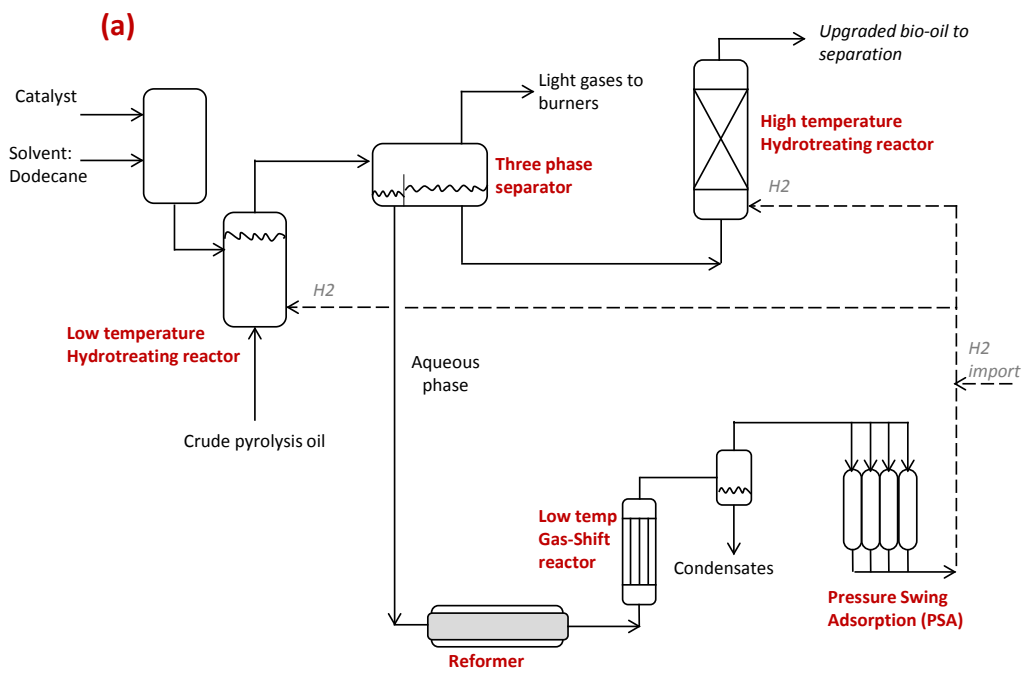
- 452 [37] Bauer LJ, Boldingh EP, inventors; Uop Llc., assignee. Use of Supported Mixed Metal Sulfides
453 for Hydrotreating Biorenewable Feeds. United States Patent WO2010005625 A3. 2010 Mar
454 4.
- 455 [38] Goudriaan F, van de Beld B, Boerefijn FR, Bos GM, Naber JE, van der Wal S, Zeevalkink JA.
456 Progress in Thermochemical Biomass Conversion. Oxford: Blackwell Science; 2001, p. 1312-
457 25.
- 458 [39] Akiya N, Savage PE. Roles of Water for Chemical Reactions in High-Temperature Water.
459 Chem Rev, 2002; 102 (8): 2725-50.
- 460 [40] Ragauskas J, Williams CK, Davison BH, Britovsek G, Cairney J, Eckert CA, Frederick Jr WJ,
461 Hallett JP, Leak DJ, Liotta CL, Mielenz JR, Murphy R, Templer R, Tschaplinski T. The path
462 forward for biofuels and biomaterials. Science, 2006; 311 (5760): 484-9.
- 463 [41] Peterson AA, Vogel F, Lachance RP, Froling M, Antal, Jr MJ, Tester JW. Thermochemical
464 biofuel production in hydrothermal media: A review of sub- and supercritical water
465 technologies. Energy Environ Sci, 2008; 1 (1): 32-65.
- 466 [42] Serrano-Ruiz JC, Dumesic JA. Catalytic routes for the conversion of biomass into liquid
467 hydrocarbon transportation fuels. Energy Environ Sci, 2011; 4 (1): 83-99.
- 468 [43] Goyal N, Pant KK, Gupta R. Hydrogen production by steam reforming of model bio-oil using
469 structured Ni/Al₂O₃ catalysts. Int J Hydrogen Energy, 2013; 38 (2): 921–33.
- 470 [44] Jones S, Zhu Y, Anderson D, Hallen R, Elliott D, Schmidt A, et al. Process Design and
471 Economics for the Conversion of Algal Biomass to Hydrocarbons: Whole Algae Hydrothermal
472 Liquefaction and Upgrading. Richland: Pacific Northwest National Laboratory (PNNL); 2014
473 March. Report No.: PNNL-23227. Contract No.: DE-AC05-76RL01830. Sponsored by the
474 Department of Energy.
- 475 [45] Sadhukhan J, Ng KS. Economic and European Union environmental sustainability criteria
476 assessment of bio-oil based biofuel systems: refinery integration cases. Ind Eng Chem Res,
477 2011; 50 (11): 6794-808.

This article should be cited as: Sharifzadeh M*, Richard CJ, Liu K, Hellgardt K, Chadwick D, Shah N. (2015). An integrated process for biomass pyrolysis oil upgrading: the synergistic approach. *Biomass & Bioenergy*. 76, 108–117, ([Link](#)).

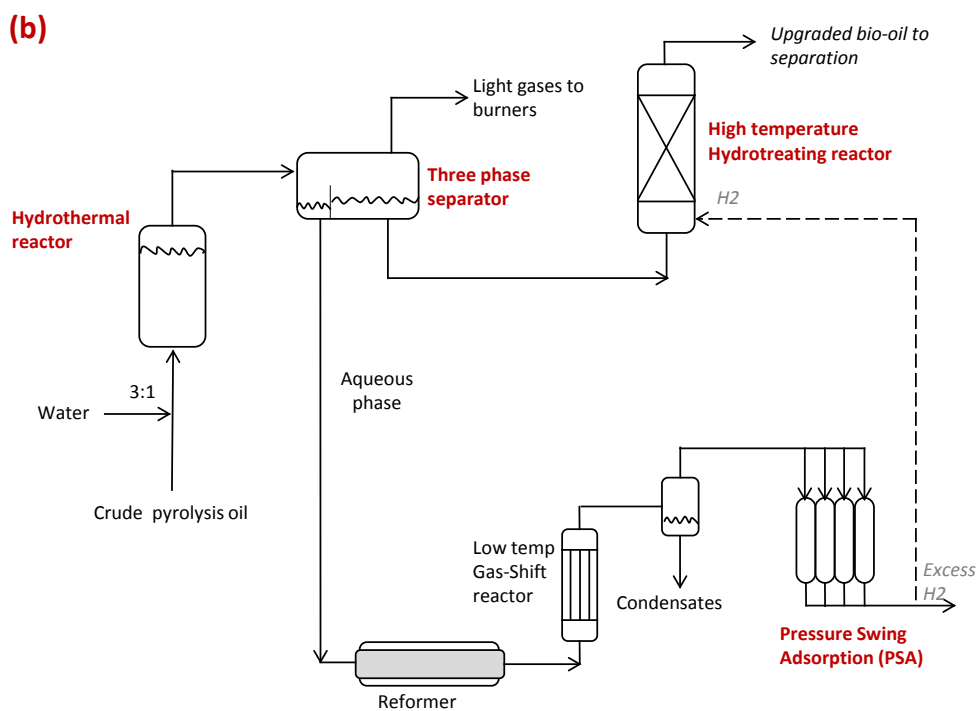
- 478 [46] Jones SB, Holladay JE, Valkenburg C, Stevens DJ, Walton CW, Kinchin C, Elliott DC, Czernik S.
479 Production of Gasoline and Diesel from Biomass via Fast Pyrolysis, Hydrotreating and
480 Hydrocracking: A Design Case. Richland: Pacific Northwest National Laboratory (PNNL); 2014
481 March. Report No.: PNNL-18284. Contract No.: DE-AC05-76RL01830. Sponsored by the
482 Department of Energy.
- 483 [47] Milne TA, Agblevor F, Davis M, Deutch S, Johnson D. Developments in Thermal Biomass
484 Conversion. London: Blackie Academic and Professional; 1997.
- 485 [48] Richard CJ, Patel B, Chadwick D, Hellgardt K. Hydrothermal deoxygenation of pyrolysis oil
486 from Norwegian spruce: *Picea abies*. *Biomass Bioenerg*, 2013 Sep; 56: 446-55.
- 487 [49] Townsend SH, Abraham MA, Huppert GL, Klein MT, Paspekt SC. Solvent Effects during
488 Reactions in Supercritical Water. *Ind Eng Chem Res*, 1988; 27 (1): 143-9.
- 489 [50] Lawson JR, Klein MT. Influence of Water on Guaiacol Pyrolysis. *Ind Eng Chem Fundam*,
490 1985; 24 (2): 203-8.
- 491 [51] Akgüla G, Kruse A. Influence of salts on the subcritical water-gas shift reaction. *J Supercrit*
492 *Fluid*, 2012 June; 66: 207–14.
- 493 [52] Matsumura Y, Nonoka H, Yokura H, Tsutsumi A, Yoshida A. Co-liquefaction of coal and
494 cellulose in supercritical water. *Fuel*, 1999; 78 (9): 1049-56.
- 495 [53] Arai K, Adschiri T, Watanabe M. Hydrogenation of Hydrocarbons through Partial Oxidation
496 in Supercritical Water. *Ind Eng Chem Res*, 2000; 39 (12): 4697-701.
- 497 [54] Phillips S, Aden A, Jechura J, Dayton D, Eggeman T. 2007, Thermochemical Ethanol via
498 Indirect Gasification and Mixed Alcohol Synthesis of Lignocellulosic Biomass. Golden:
499 National Renewable Energy Laboratory (NREL); April 2007, Report No.: NREL/TP-510-41168.
500 Contract No. DE-AC36-99-GO10337. Sponsored by the Department of Energy.
- 501 [55] Natural Gas Prices [Internet]. Washington: US Energy Information Administration US
502 Department of Energy; c2008-13 [updated 2015 Jan 30; cited 2015 Feb 7]. Available
503 from: http://www.eia.gov/dnav/ng/ng_pri_sum_dcu_nus_a.htm

This article should be cited as: Sharifzadeh M*, Richard CJ, Liu K, Hellgardt K, Chadwick D, Shah N. (2015). An integrated process for biomass pyrolysis oil upgrading: the synergistic approach. *Biomass & Bioenergy*. 76, 108–117, ([Link](#)).

- 504 [56] Electricity Wholesale Market [Internet]. Washington: US Energy Information
505 Administration; US Department of Energy c2001-15 [updated 2015 Feb 5; cited 2015 Feb 7].
506 Available from: <http://www.eia.gov/electricity/wholesale/>
- 507 [57] Aspen Plus software tool, V8.4. Aspen Tech.
- 508 [58] Weekly Retail Gasoline and Diesel Prices [Internet]. Washington: US Energy Information
509 Administration; US Department of Energy c2009-14 [updated 2015 Feb 2; cited 2015 Feb 7].
510 Available from: http://www.eia.gov/dnav/pet/pet_pri_gnd_dcus_nus_a.htm
- 511 [59] Bimbela, F, Oliva M, Ruiz J, Garcia L, Aruzo J. Steam reforming of bio-oil fractions for syngas
512 production and energy. *Env Eng Sci*, 2011; 28 (11): 757-63
- 513 [60] Seyedeyn-Azad F, Abedi J, Sampouri, S. Catalytic steam reforming of aqueous phase of bio-
514 oil over Ni-based alumina supported catalysts. *Ind Eng Chem Res*, 2014; 53 (46): 17937-44.
515



516



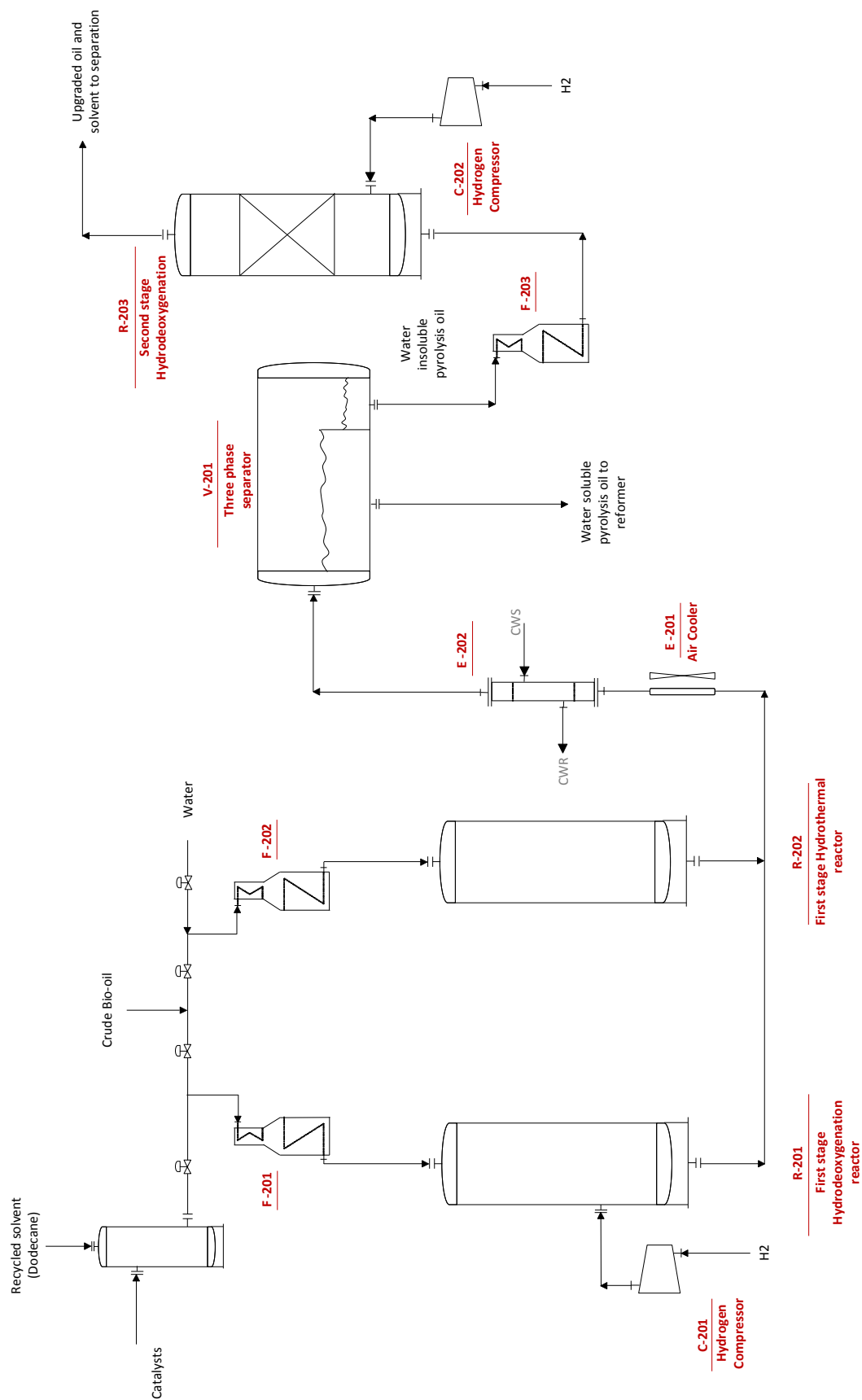
517

518 Fig. 1 - Simplified process modelling for calculating Key Process Indicators (KPIs): (a) liquid-phase

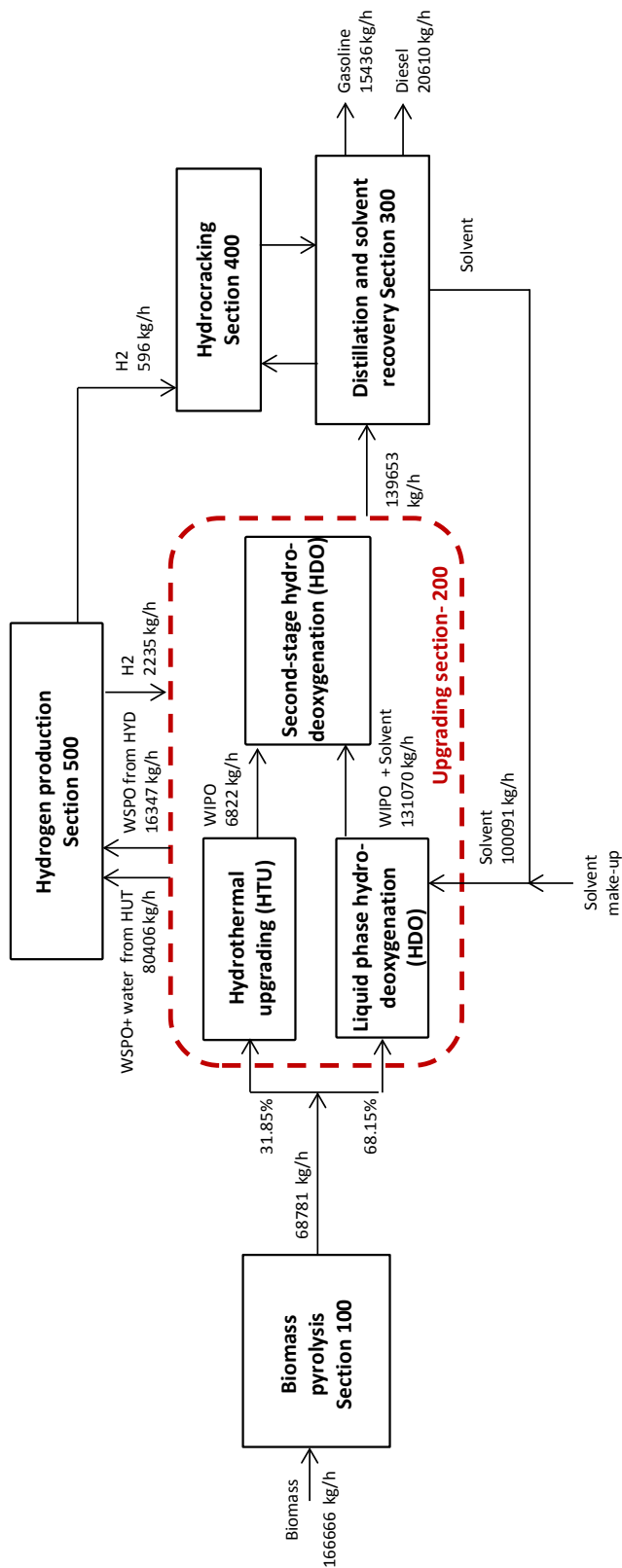
519

hydrodeoxygenation, (b) near critical hydrothermal treatment.

520

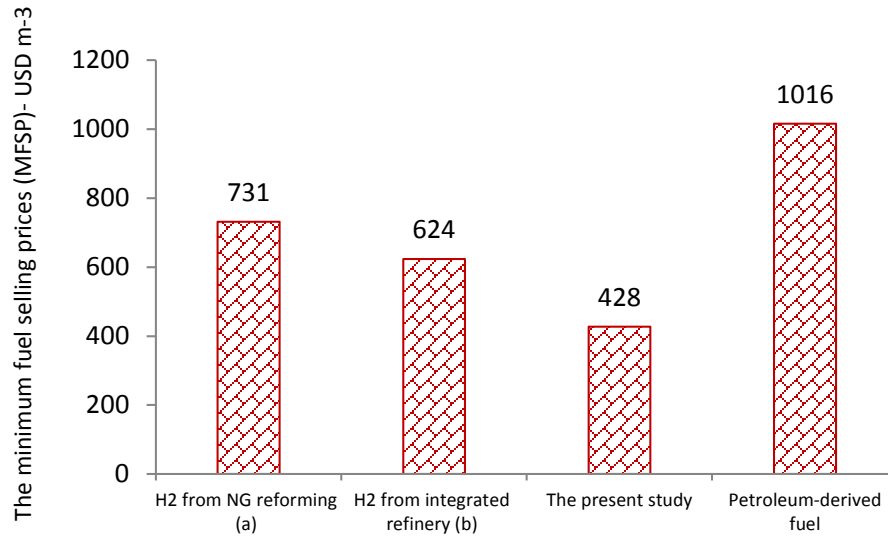


522 Fig. 2 - Integrated catalytic upgrading of pyrolysis oil (PO): adjusting Valves 201-204 allows
 523 optimization of the product yields.



525 **Fig. 3 - Process block diagrams for new process including the proposed integrated upgrading**

526 **section**



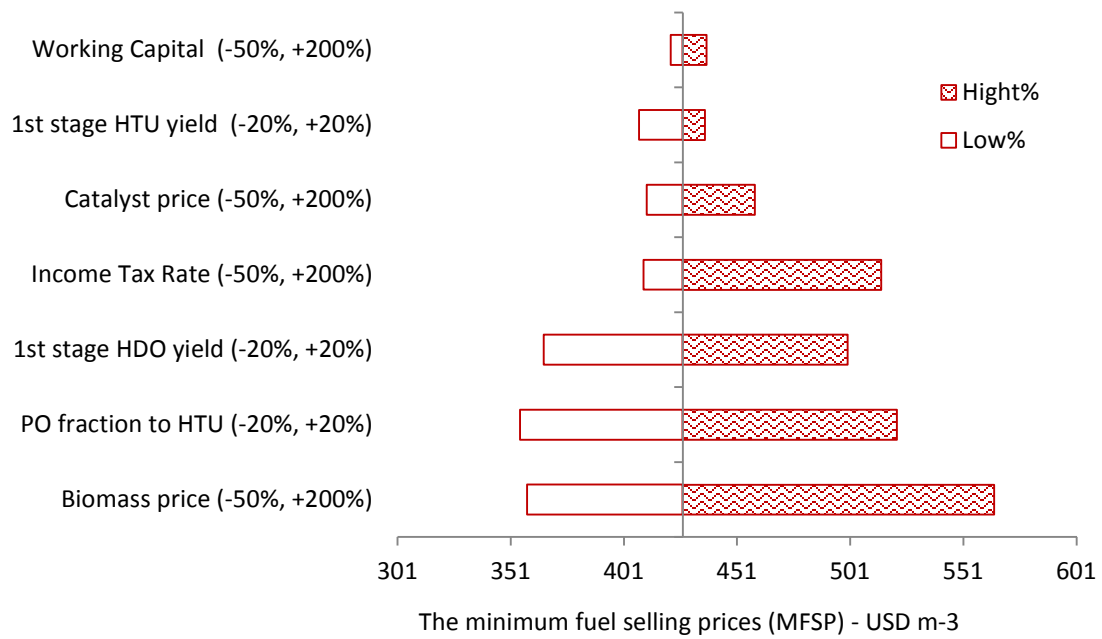
527

528 **Fig. 4 - The minimum fuel selling price (MFSP), in comparison to the benchmarks from literature-**

529 **2012).**

530

This article should be cited as: Sharifzadeh M*, Richard CJ, Liu K, Hellgardt K, Chadwick D, Shah N. (2015). An integrated process for biomass pyrolysis oil upgrading: the synergistic approach. *Biomass & Bioenergy*. 76, 108–117, ([Link](#)).



531

532

Fig. 5 - The sensitivity of the minimum fuel selling price (MFSP) with respect to key process

533

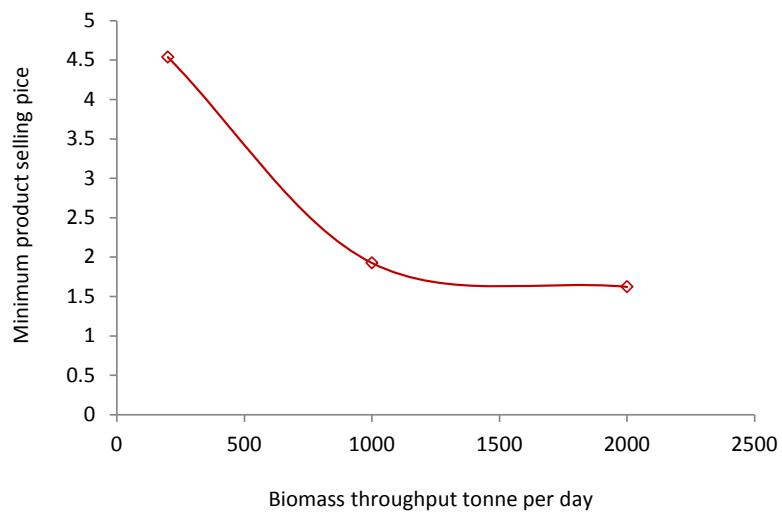
variables

534

535

536

This article should be cited as: Sharifzadeh M*, Richard CJ, Liu K, Hellgardt K, Chadwick D, Shah N. (2015). An integrated process for biomass pyrolysis oil upgrading: the synergistic approach. *Biomass & Bioenergy*. 76, 108–117, ([Link](#)).



537

538

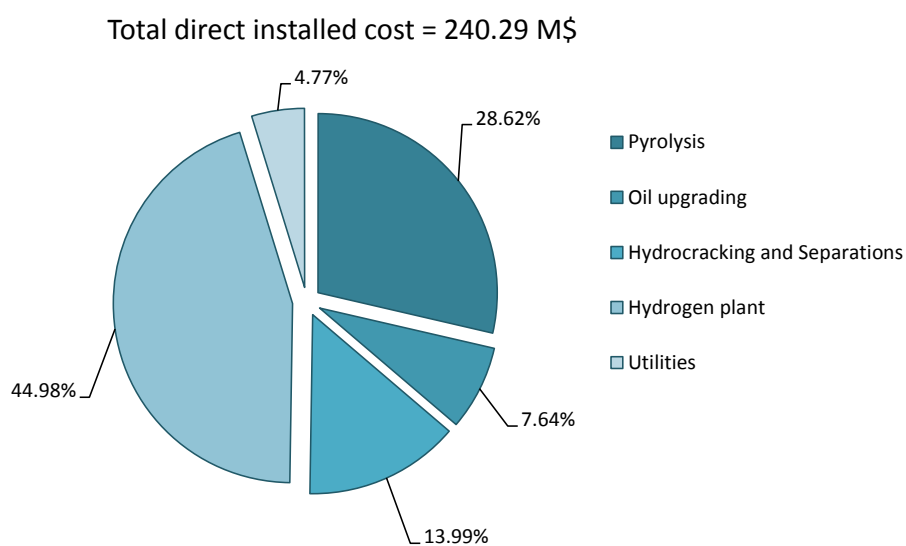
Fig. 6. The sensitivity of the minimum fuel selling price (MFSP) with respect to process scale

539

(biomass throughput)

540

This article should be cited as: Sharifzadeh M*, Richard CJ, Liu K, Hellgardt K, Chadwick D, Shah N. (2015). An integrated process for biomass pyrolysis oil upgrading: the synergistic approach. *Biomass & Bioenergy*. 76, 108–117, ([Link](#)).

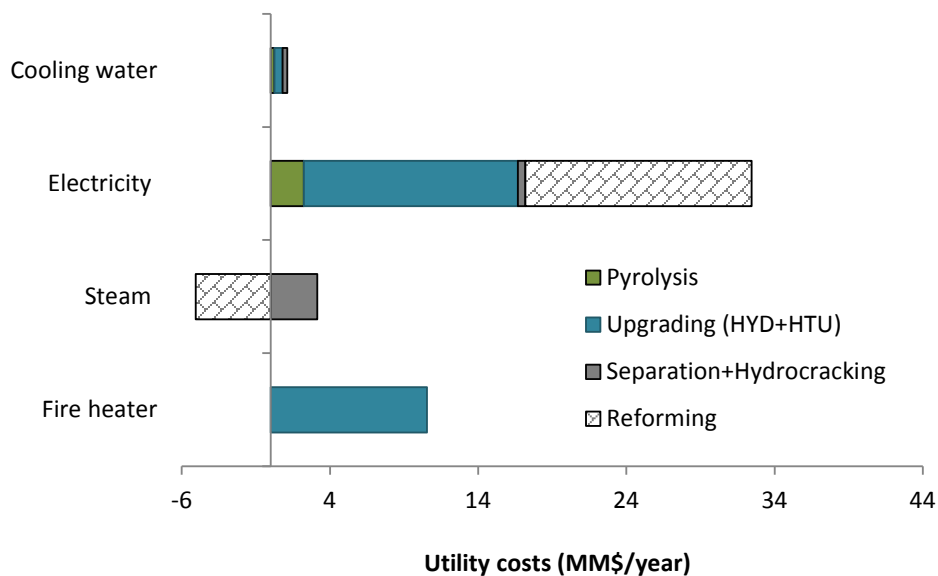


541

542

Fig. 7 - The required capital investment for different processing sections.

543



544

545

Fig. 8 - The contribution of the sub-processes to the costs of utilities.

546

547

This article should be cited as: Sharifzadeh M*, Richard CJ, Liu K, Hellgardt K, Chadwick D, Shah N. (2015). An integrated process for biomass pyrolysis oil upgrading: the synergistic approach. *Biomass & Bioenergy*. 76, 108–117, ([Link](#)).

Table 1. Composition of pyrolysis oil (mass fraction)

C	H	O	Water
0.4010	0.0825	0.5165	0.3335

548

549

This article should be cited as: Sharifzadeh M*, Richard CJ, Liu K, Hellgardt K, Chadwick D, Shah N. (2015). An integrated process for biomass pyrolysis oil upgrading: the synergistic approach. *Biomass & Bioenergy*. 76, 108–117, ([Link](#)).

Table 2. Elemental analysis of water insoluble bio oil from hydrothermal processing at 380°C

Time ^a (min)	C (mass fraction)	H (mass fraction)	O (mass fraction)
0	0.63	0.07	0.30
1	0.66	0.07	0.27
10	0.70	0.07	0.23

550 ^a time at 380°C; heat up time = 5 min
551

This article should be cited as: Sharifzadeh M*, Richard CJ, Liu K, Hellgardt K, Chadwick D, Shah N. (2015). An integrated process for biomass pyrolysis oil upgrading: the synergistic approach. *Biomass & Bioenergy*. 76, 108–117, ([Link](#)).

Table 3. Hydrodeoxygenation of pyrolysis oil at 250°C using NiMo nanosulphide catalyst

Carbon in water phase (mass fraction)	Oxygen in solvent phase (mass fraction)	Oxygen in residue (mass fraction)	Estimated Organo Oxygen removal (mass fraction)
0.113	0.166	0.277	0.20

552

This article should be cited as: Sharifzadeh M*, Richard CJ, Liu K, Hellgardt K, Chadwick D, Shah N. (2015). An integrated process for biomass pyrolysis oil upgrading: the synergistic approach. *Biomass & Bioenergy*. 76, 108–117, ([Link](#)).

Table 4. Key process indicators (KPIs)

Key process indicators (KPIs)	HTU	HDO
Fuel: Pyrolysis oil (mass ratio)	0.3228	0.6520
H2 required: Pyrolysis oil (mass ratio)	0.0117	0.0422
H2 produced : Pyrolysis oil (mass ratio)	0.0659	0.0169
Net H2 requirement : Pyrolysis oil (mass ratio)	0.0542	-0.0254
Solvent : Pyrolysis oil (mass ratio)	2.98 (water)	2.14 (dodecane)

553

554

This article should be cited as: Sharifzadeh M*, Richard CJ, Liu K, Hellgardt K, Chadwick D, Shah N. (2015). An integrated process for biomass pyrolysis oil upgrading: the synergistic approach. *Biomass & Bioenergy*. 76, 108–117, ([Link](#)).

Table 5. Summary of variable operating cost

Materials/Chemicals/Utilities	Cost	Unit	Reference
Biomass	0.0552	\$ kg ⁻¹	[46]
Natural gas	0.137373309	\$ m ⁻³	[55]
Catalyst	7% of Fuel price		[46]
Electricity	37.02	\$ MWh ⁻¹	[56]
Disposal of ash	0.0198	\$ kg ⁻¹	[46]
Steam ^a	1.9 -4.5	\$ GJ ⁻¹	[57]
Cooling water	0.212	\$ GJ ⁻¹	[57]

555 *Note:* ^a varied for steam with different pressure; b varied for different types of refrigerant.

An Integrated Process for Biomass Pyrolysis Oil Upgrading: A Synergistic Approach

M. Sharifzadeh^{a*}, C. J. Richard^b, K. Liu^b, K. Hellgardt^b, D. Chadwick^b and N. Shah^a

^a Centre for Process Systems Engineering (CPSE), Department of Chemical Engineering, Imperial College London.

^b Department of Chemical Engineering, Imperial College London

Electronic Supplementary Material

The presented materials include the details of the experimental procedures and summary of the results. In addition, this document report additional information regarding process modelling including the flow diagrams and descriptions of Sections 100-500 (in Fig. 3 of the manuscript), and the assumptions used for modelling each section.

Experimental procedures and summary of results

A set of five stainless steel batch reactors (volume: 8.0 cm³ and 12.7 mm bore) were used for all experiments according to a previously reported method ^[S1]. These were constructed of stainless steel tubing and sealed at each end using a gas sampling valve and compression fittings (Swagelok®). The empty batch reactors were weighed initially and charged with deionised water (3g) and pyrolysis oil (1g). The batch reactors were then purged with argon to remove air, sealed and weighed a second time. They were then heated in an air recirculating oven to a reaction temperature of 380°C. The residence times were: $t_0 = 0$ (taken as time when reaction temperature was reached) $t_1 = 1$; $t_2 = 2$; $t_5 = 5$; $t_{10} = 10$ minutes. It required 5 minutes (*i.e.*, t_0) to reach the reaction temperature of 380°C. After heating to the required residence time, the batch reactors were immediately quenched in ice and left to stand for several hours to maximise any phase separation of water, gas and char. After each reaction, the loaded reactors were externally dried and then reweighed a third time to confirm no potential mass loss occurred due to leakage. Water soluble pyrolysis oil was separated, weighed and stored for analysis. The remaining oil was then washed out of the reactors with acetone and all the acetone washings stored. The acetone insoluble char was collected and weighed. Any char which could not be collected was determined by calculating the difference between the weights of the emptied initial and post reaction batch reactors. A GC-TCD was used to analyse for CO, CO₂, H₂ and CH₄.

Table 1 (in the manuscript) shows the elemental analysis of the pyrolysis oil. Table S1 reports the mass yield of each phase for hydrothermal experiment at different residence times. Table S2 reports the total organic carbon and carbon yield of water soluble pyrolysis oil for different residence times. The elemental analyses of water insoluble pyrolysis oil for the hydrothermal experiments are reported in Table 2 (in the manuscript) and the compositions of gas products from hydrothermal experiment are reported in Table S3. Table S4 reports the composition of the water soluble product using GCMS.

The GC-MS analysis of all samples was carried out at the Mass Spectrometry Facility at King's College London using an Agilent 6890/5973 Mass Selective Detector GC-MS equipped with a 30 m x 0.25 mm x 250 µm HP-5MS column. The program parameters were 50°(1 min)-10°/min-320° (10 min). 4-methyl valeric acid and tridecane were used as internal standards for the aqueous and non-aqueous fractions respectively.

CHN analysis was done at the University of Sheffield Microanalysis service using a Perkin Elmer 2400 CHNS/O Series II Elemental Analyser. The CHM analysis of each sample was the average of three determinations. The oxygen content was determined by mass balance. The results are accurate to ±0.3% of the total mass of sample. TOC analysis was done by Intertek Sunbury Technology Centre (UK). Water content of the pyrolysis oil was done by Karl Fischer coulometric titration using a Mettler Toledo C20X instrument.

The experimental procedure for hydrodeoxygenation is reported in the manuscript. Table S4 reports the mass balance for the hydrodeoxygenation experiment. Table S6 reports the composition of water soluble pyrolysis oil (WSPO) in the hydrodeoxygenation experiment. Table S7 reports the composition of water insoluble pyrolysis oil (WIPO) in the hydrodeoxygenation experiment.

Table S1. The mass balance for hydrothermal experiments

Time [min]	Initial pyrolysis oil	WSBO	WIBO	Char	Gas
t0=0	1.01	3.7027	0.31427	0.001	0
t1=1	1.00	3.6727	0.3354	0.0009	0.002005522
t10=10	1.08	3.6823	0.32143	0.0193	0.000923392

Table S2. Total organic carbon and carbon yield of water soluble pyrolysis oil for different residence time for the hydrothermal experiments

Time [min]	TOC	C in WSBO/C in PO [%]
t0=0	4.8	40.4
t1=1	3.8	32.9
t2=2	3.3	28.8
t5=5	3.0	26.3
t10=10	2.8	22.2

Table S4. The composition (mass fractions) of water soluble pyrolysis oil (WSPO) analysed by GCMS for the hydrothermal experiments.

Compound	Oil E		
	t0=5	t1=6	t10=15
Time (min)	mass fraction	mass fraction	mass fraction
2-Butanone, 1-hydroxy-	0.0021	0.0030	0.0001
Acetic acid	0.0222	0.0356	0.0040
Furfural	0.0062	0.0100	0.0000
Formic acid	0.0000	0.0000	0.0000
Ketone, 2-furyl methyl	0.0000	0.0000	0.0000
Propanoic Acid	0.0032	0.0054	0.0008
Butanoic Acid	0.0010	0.0015	0.0002
Butanoic acid, 4-hydroxy-	0.0008	0.0011	0.0001
2(5H)-Furanone, 3-methyl-	0.0016	0.0020	0.0001
2-Cyclopenten-1-one, 2-hydroxy-3-methyl-	0.0050	0.0070	0.0006
Guaiacol	0.0074	0.0093	0.0001
trans-2-Pentenoic acid	0.0008	0.0013	0.0000
4-Methyl-5H-furan-2-one	0.0011	0.0018	0.0001
p-Cresol, 2-methoxy-	0.0055	0.0070	0.0006
Phenol	0.0019	0.0026	0.0002
2-Hydroxy-gamma-butyrolactone	0.0002	0.0000	0.0000
Levulinic acid	0.0023	0.0051	0.0008
HMF	0.0114	0.0151	0.0000
Vanillin	0.0046	0.0048	0.0002
Acetophenone, 4'-hydroxy-3'-methoxy-	0.0023	0.0000	0.0000
Guaiacylacetone	0.0017	0.0025	0.0000
Pyrocatechol	0.0033	0.0043	0.0004
4-((1E)-3-Hydroxy-1-propenyl)-2-methoxyphenol	0.0009	0.0006	0.0000
Benzeneacetic acid, 4-hydroxy-3-methoxy-	0.0032	0.0038	0.0004
1,4-Benzenediol	0.0014	0.0018	0.0002
Water	0.9099	0.8745	0.9910
Total	1	1	1

Table S6. The composition (mass fractions) of water soluble pyrolysis oil (WSPO) analysed by GCMS for the hydrodeoxygenation experiments.

Compound	CAS Number	Mol Formula	Mass fraction
Acetaldehyde	75-07-0	C2H4O	0.00023
Acetone	67-64-1	C3H6O	0.00108
Acetic acid, methyl ester	79-20-9	C3H6O2	0.00014
2-Butanone	78-93-3	C4H8O	0.00089
Ethanol	64-17-5	C2H6O	0.02876
2,3-Butanedione	431-03-8	C4H6O2	0.00007
Pentanoic acid, methyl-	624-24-8	C6H12O2	0.00017
Cyclopentanone	120-92-3	C5H8O	0.00089
Acetoin	513-86-0	C4H8O2	0.00741
2-Propanone, 1-hydroxy-	116-09-6	C3H6O2	0.00456
Propanoic acid, 2-hydroxy-	97-64-3	C3H6O3	0.00438
1-Hydroxy-2-butanone	5077-67-8	C4H8O2	0.00266
Hydroxy Acetic acid	79-14-1	C2H4O3	0.00111
Acetic acid	64-19-7	C2H4O2	0.03624
Furfural	98-01-1	C5H4O2	0.00004
2-Furanmethanol, tetra...	97-99-4	C5H10O2	0.00235
Formic acid	64-18-6	CH2O2	0.00001
2-Acetylfuran	1192-62-7	C6H6O2	0.00196
2,5-Hexanedione	110-13-4	C6H10O2	0.00579
Propanoic acid	79-09-4	C3H6O2	0.00480
Propanoic acid, 2-methyl-	79-31-2	C4H8O2	0.00047
Pentanoic acid, 4-oxo-ethyl ester	539-88-8	C7H12O3	0.00144
3,6-Heptanedione	1703-51-1	C7H12O2	0.00128
1,2-Propanediol, 2-acetate	627-69-0	C5H10O3	0.00059
1,2-Ethanediol	107-21-1	C2H6O2	0.00186
Butanoic acid	107-92-6	C4H8O2	0.00744
1,2-Ethanediol, monoacetate	542-59-6	C4H8O3	0.01539
Butyrolactone	96-48-0	C4H6O2	0.00382
2-Furanone, 2,5-dihydro-3,5-dimethyl	35298-48-7	C6H8O2	0.00011
Propanoic acid, 2-hydroxy-	503-66-2	C3H6O3	0.00124
2-Butenoic acid, (E)-	107-93-7	C4H6O2	0.00003
Crotonic acid	107-93-7	C4H6O2	0.00014
2-Cyclopenten-1-one, 2 methyl?	1120-73-6	C6H8O	0.00005
2-Pentenoic acid	13991-37-2	C5H8O2	0.00014
Phenol, 2-methoxy-	90-05-1	C7H8O2	0.00948
4-Methyl-5H-furan-2-one	6124-79-4	C5H6O2	0.00081
Succinic anhydride	108-30-5	C4H4O3	0.00104
Creosol	93-51-6	C8H10O2	0.00518
Phenol, 2-methyl-	95-48-7	C7H8O	0.00102
Phenol	108-95-2	C6H6O	0.00361
Phenol, 4-ethyl-2-methoxy-	2785-89-9	9H12O2	0.00178
Carvenone	499-74-1	C10H16O	0.00053
Valeric anhydride	2082-59-9	C10H18O3	0.00006
2-HYDROXY-GAMMA-BUTYROLACTONE	19444-84-9	C4H6O3	0.00097
2(3H)-Furanone, 3-acetyldihydro	517-23-7	C6H8O3	0.00050
Ethyl hydrogen succinate	1070-34-4	C6H10O4	0.00035
4-Acetylbutyric acid	3128-06-1	C6H10O3	0.00010
(R)-5-Hydroxymethyl-dihydrofuran-2-one	52813-63-5	(C5H8O3)	0.00752
1,3-Cyclopentanedione	3859-41-4	C5H6O2	0.00052
Vanillin	121-33-5	C8H8O3	0.00016
Isoeugenol	97-54-1	C10H12O2	0.00002
Apocynin	498-02-2	C9H10O3	0.00430
2-Cyclopenten-1-one,3-methyl?	2758-18-1	C6H8O	0.00048
Acetophenone, 4'-hydroxy-	99-93-4	C8H8O2	0.00014
Hydroquinone	123-31-9	C6H6O2	0.00048
Water		H2O	0.77938
Unidentified			0.04403

Table S3. Composition of gas products from hydrothermal experiments

time(min)	vol (ml/g-oil)	CH ₄ (vol/vol %)	H ₂ (vol/vol %)	CO (vol/vol %)	CO ₂ (vol/vol %)
0	0	0	0	0	0
1	1.3	5.4	23.9	69.0	1.6
2	3.5	5.9	20.5	73.0	0.5
5	2.6	7.9	19.5	71.0	1.7
10	11.9	5.9	28.1	62.5	3.5

Table S5. The mass balance for the hydrodeoxygenation experiments

Initial pyrolysis oil	Dodecane (solvent)	WIBO + Solvent	WSBO	Char	Gas
7.06412	0.0000	16.43312	2.35790	Negligible	n.d.*
7.02025	7.0653	16.98718	1.78247	Negligible	n.d.
6.99809	14.0136	16.71169	2.02594	Negligible	n.d.

* Not determined

Table S7. The composition (mass fractions) of water insoluble pyrolysis oil (WSPO) analysed by GCMS for the hydrodeoxygenation experiments.

Compound	CAS Number	Mol Formula	Mass fraction
Dodecane (Solvent)	112-40-3	C ₁₂ H ₂₆	0.9168
Dimethyl ether	115-10-6	C ₂ H ₆ O	0.000055
Ethanol	64-17-5	C ₂ H ₆ O	0.000358
Furan	110-00-9	C ₄ H ₄ O	0.000128
Methyl acetate	79-20-9	C ₃ H ₆ O ₂	0.000264
Propionic acid, ethyl ester	105-37-3	C ₅ H ₁₀ O ₂	0.000086
Diethyl acetal	105-57-7	C ₆ H ₁₄ O ₂	0.000054
1-Hydroxy-2-butanone	5077-67-8	C ₄ H ₈ O ₂	0.001068
Cyclopentanone	120-92-3	C ₅ H ₈ O	0.000846
Furan, 2-ethyl-5-methyl-	1703-52-2	C ₇ H ₁₀ O	0.000119
Cyclopentanone, 2-methyl-	1120-72-5	C ₆ H ₁₀ O	0.000059
2-Methyl-2-cyclopentenone	1120-73-6	C ₆ H ₈ O	0.000495
Phenol	108-95-2	C ₆ H ₆ O	0.001285
p-Cresol, 2-methoxy-	93-51-6	C ₈ H ₁₀ O ₂	0.000016
2-Methyl-1-phenyl-1-pentanol	73177-67-0	C ₁₂ H ₁₈ O	0.000516
p-Ethylguaiaicol	2785-89-9	C ₉ H ₁₂ O ₂	0.009510
Guaiaicylpropane	2785-87-7	C ₁₀ H ₁₄ O ₂	0.064159
Vanillin	121-33-5	C ₈ H ₈ O ₃	0.000770
(E)-Isoeugenol	97-54-1	C ₁₀ H ₁₂ O ₂	0.000158
Acetoguaiaicon	498-02-2	C ₉ H ₁₀ O ₃	0.000000
Guaiaicylacetone	2503-46-0	C ₁₀ H ₁₂ O ₃	0.000127
2-Naphthol, 3-methoxy-	18515-11-2	C ₁₁ H ₁₀ O ₂	0.000448
Dibenzo[b,d]cycloheptanone, 1,2,9-trimethoxy-	-	C ₁₈ H ₁₈ O ₄	0.002712
Total			1.0000

Process modelling

The overall process diagram is shown in Fig. S1. (identical to Fig. 3). The following sections will present the process description of sub-processes (100-500) and their processing steps. The applied modelling techniques and underlying assumptions are discussed in the following.

Section 100: Biomass pyrolysis

Fig. S2, adapted from Jones, *et al.*,^[S1] shows the process flow diagram for the pyrolysis section. In this section, the grinded biomass is firstly dried and then fed to a short residence time (< 1 second) circulating fluidized bed reactor (R-101) where it is converted to a widespread range of components which can be roughly classified into non-condensable gases, condensable gases and char. Sand acts as the fluidization and heating medium, and together with char are separated at Cyclone-101. The char is burned in the combustor (E-101) in order to heat the circulating sand which in turn will supply the required energy for the endothermic pyrolysis reactions. The reaction effluents are quickly quenched in order to suppress undesirable reactions, which otherwise would degrade the products in favour of char and light gases. A fraction of light gases are also burned in the combustor and the rest are recycled to the reactor. The condensable products of pyrolysis reactions form a brownish mixture which contains significant amount of oxygenates and is chemically unstable. Furthermore, it has lower energy content and is immiscible with the petroleum fuel. Therefore, it is sent to Section 200 for upgrading.

Section 200: integrated pyrolysis oil upgrading

As shown in Figure S3, and extensively discussed in the manuscript, a new reaction network was developed for upgrading the pyrolysis oil. In the new process, firstly the pyrolysis oil is split between two first-stage upgrading reactors. The split fraction is an optimization variable in order to minimize the hydrogen requirements. The fraction of pyrolysis oil sent for hydrothermal upgrading is firstly mixed with water and then sent to the hydrothermal reactor (R-202) at near-supercritical conditions (350°C and 200bar). The rest of the pyrolysis oil is firstly mixed with the dodecane solvent and then fed into a trickle flow reactor (R-201) where it reacts with hydrogen. The effluents of both first-stage upgrading reactors are cooled and phase separated. The water insoluble pyrolysis oil (WIPO) is sent to the second-stage hydrodeoxygenation reactor (R-203) where hydrodeoxygenation reactions remove any remaining oxygen from the fuel. The water soluble pyrolysis oil (WSPO) is sent to the reformer for hydrogen production in Section 500.

Section 300 and 400: Separation and hydrocracking

The flow diagram for Sections 300 and 500 is shown in Fig. S4. The upgraded effluent are further refined in Section 300 through a sequence of distillation columns. The dissolved light gases are separated in Column T-301 and sent to Section 600 for hydrogen production. Then, the naphtha fraction is separated in Column T-302. The boiling point of the dodecane solvent overlaps with the boiling range of the biodiesel product. Therefore, two distillation columns were considered. A fraction of diesel, which is lighter than the dodecane solvent, is separated from the top of Column T-303 and the heavier fraction is separated from the bottom of Column T-304. The overhead of Column T-304 mostly consists of the dodecane solvent and is recycled to the first-stage hydrodeoxygenation reactor. Separation section is also integrated to a hydrocracker reactor (R-401), where heavy-ends are converted to higher-value lighter products.

Section 500: Hydrogen production

The process flow diagram is shown in Fig. S5, Jones, *et al.*,^[S2]. The water soluble pyrolysis oil (WSPO) from Upgrading Section was used in the reformer (R-501) where it is converted to the syngas, a mixture of carbon oxides, hydrogen, and water. The overall hydrogen yield is further improved in a low temperature reactor, before being sent to the pressure swing adsorption (PSA) for separation. The tail gas (CO, CO₂ and unseparated hydrogen) is recycled to the reformer and burned in the combustion zone. The excess heat is used for producing steam.

Process modelling and implementation considerations

The process throughput was 2000 ton per day hybrid poplar, similar to Jones, et al.'s study [S1]. The process modelling was conducted using Aspen plus™ simulator. The required information for modelling Pyrolysis Section and Hydrogen Production Section were adapted from [S2]. The required information for modelling reactors in Upgrading Section were modelled based on the yield results from the experimental program as reported in Tables S1-S7. In modelling Separation Section (300), the specifications of the distillations columns were adjusted so the gasoline and diesel products have the same quality as [S2]. The hydrocracking yield in Section 500 was also adopted from this study. The operating conditions are summarized in Table S8. The distillation columns were modelled using RADFRAC unit operation in Aspen Plus. The pressure swing adsorption was modelled using "SEP" unit operation in Aspen Plus™, assuming 90% separation efficiency. The costs of conventional unit operations (e.g., distillations, compressors) were evaluated using Aspen Economic Analyzer™. The costs of nonconventional unit operations (e.g., reformer, pyrolyzer) were calculated by scaling with respect to economic data [S2].

Table S8. The modelling approach and operating conditions for major reactors.

Reactor	Description	T (C)	P (MPa)	Modelling approach	Ref.
R101 (Fig S2)	Pyrolysis reactor	500	0.108219	Yield	[S2]
R201 (Fig S3)	First stage Hydrodeoxygenation reactor	250	5	Yield	Experimental results
R202 (Fig S3)	First stage Hydrothermal upgrading reactor	380	22	Yield	Experimental results
R203 (Fig S3)	Second stage Hydrodeoxygenation reactor	251	17.2	Yield	[S2]
R401 (Fig S4)	Hydrocracker	675	8.9	Yield	[S2]
R701 (Fig S5)	Reformer reactor	850	2.6	Chemical Equilibrium	[S2]
R-702 (Fig S5)	High temperature gas shift reactor	353	2.5	Conversion (80% CO)	[S2]

Reference

[S1] C.J.Richard, B.Patel, D.Chadwick, K.Hellgardt, (2013). *Biomass and Bioenergy*, 56, 446-455.

[S2] S.B. Jones, J.E. Holladay, C. Valkenburg, D.J. Stevens, C.W. Walton, C. Kinchin, D.C. Elliott, S. Czernik. Production of Gasoline and Diesel from Biomass via Fast Pyrolysis, Hydrotreating and Hydrocracking: A Design Case. US Department of Energy 2009; Technical Report.

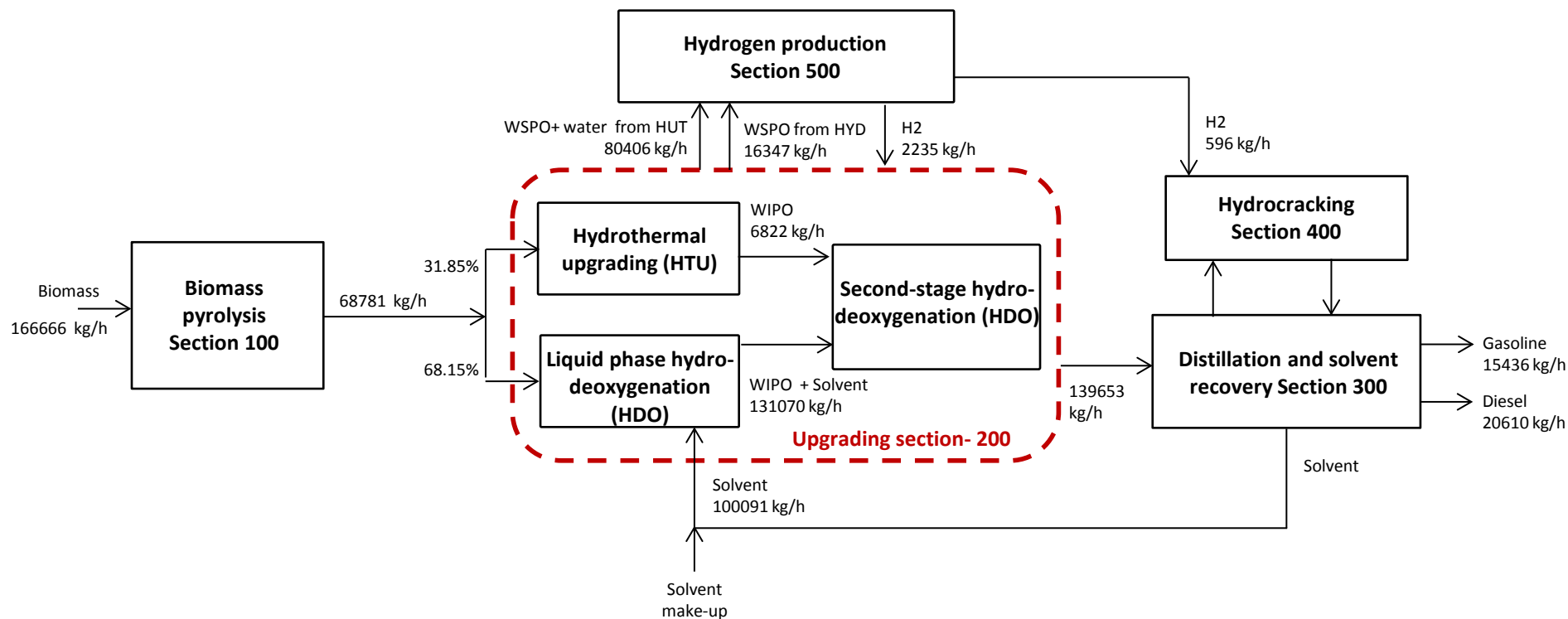


Fig. S1. The overall process block diagram - this figure is identical to Fig 3 in the manuscript.

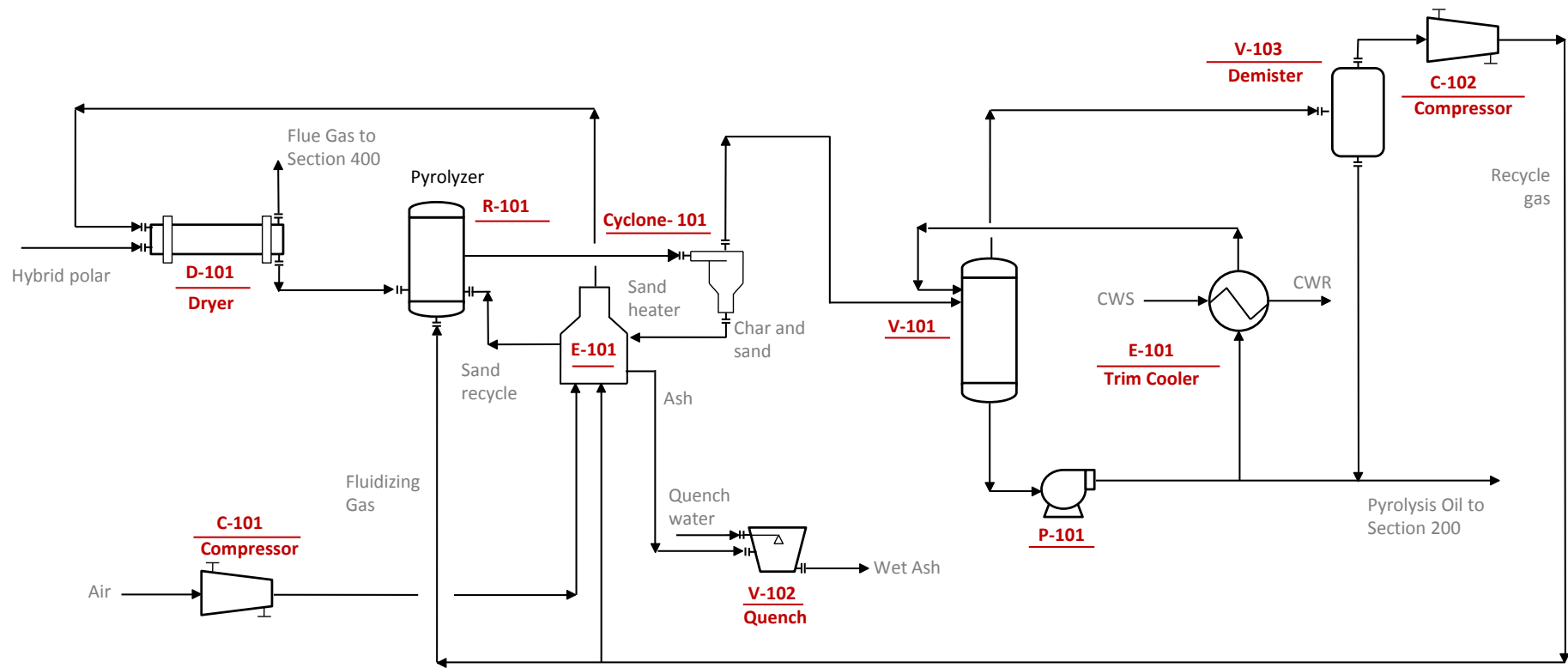


Fig. S2. Biomass Pyrolysis Section (100) - adapted from Jones, *et al.*, [51]

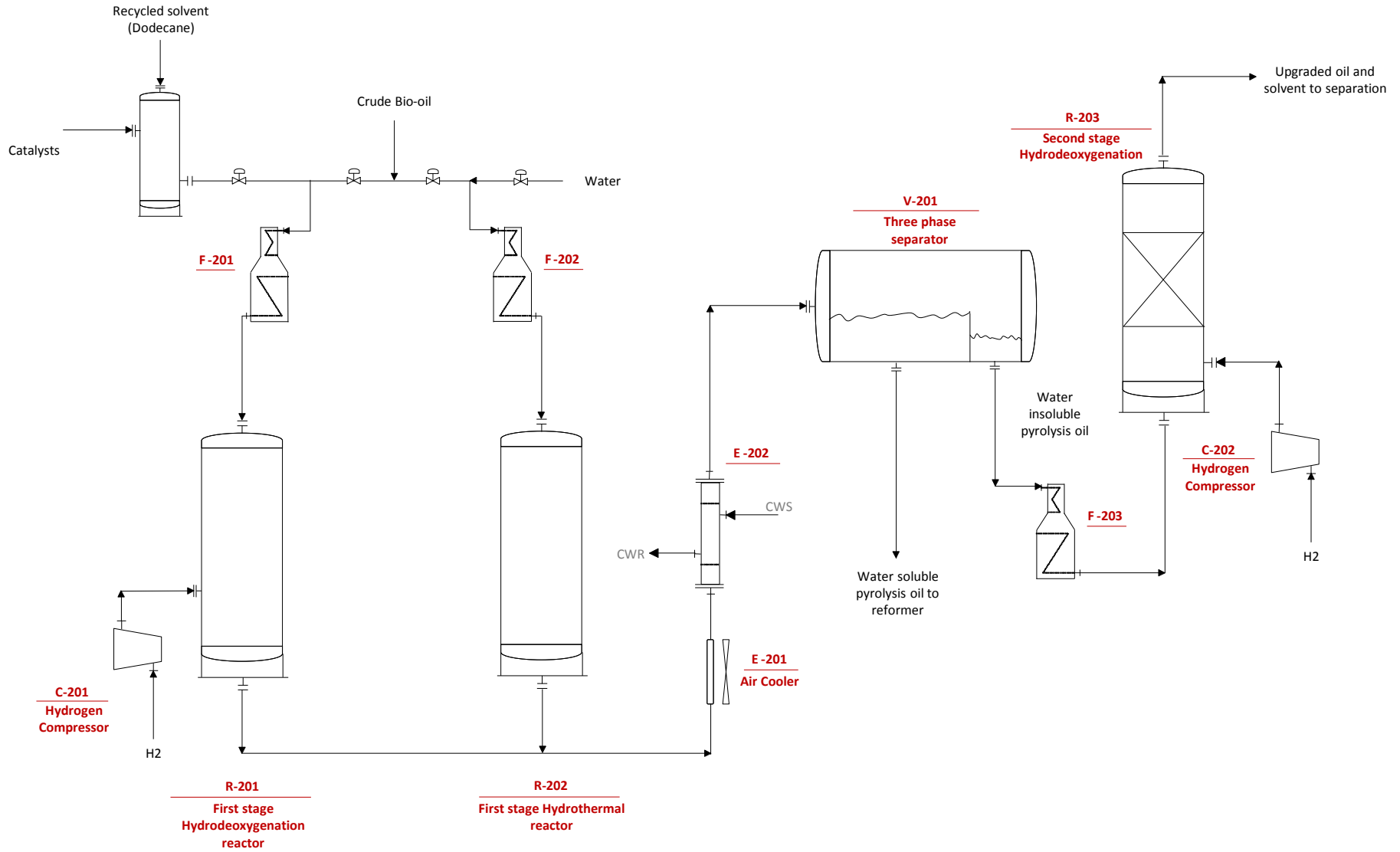


Fig. S3. Pyrolysis oil Upgrading Section (200) - this figure is identical to Fig 2 in the manuscript.

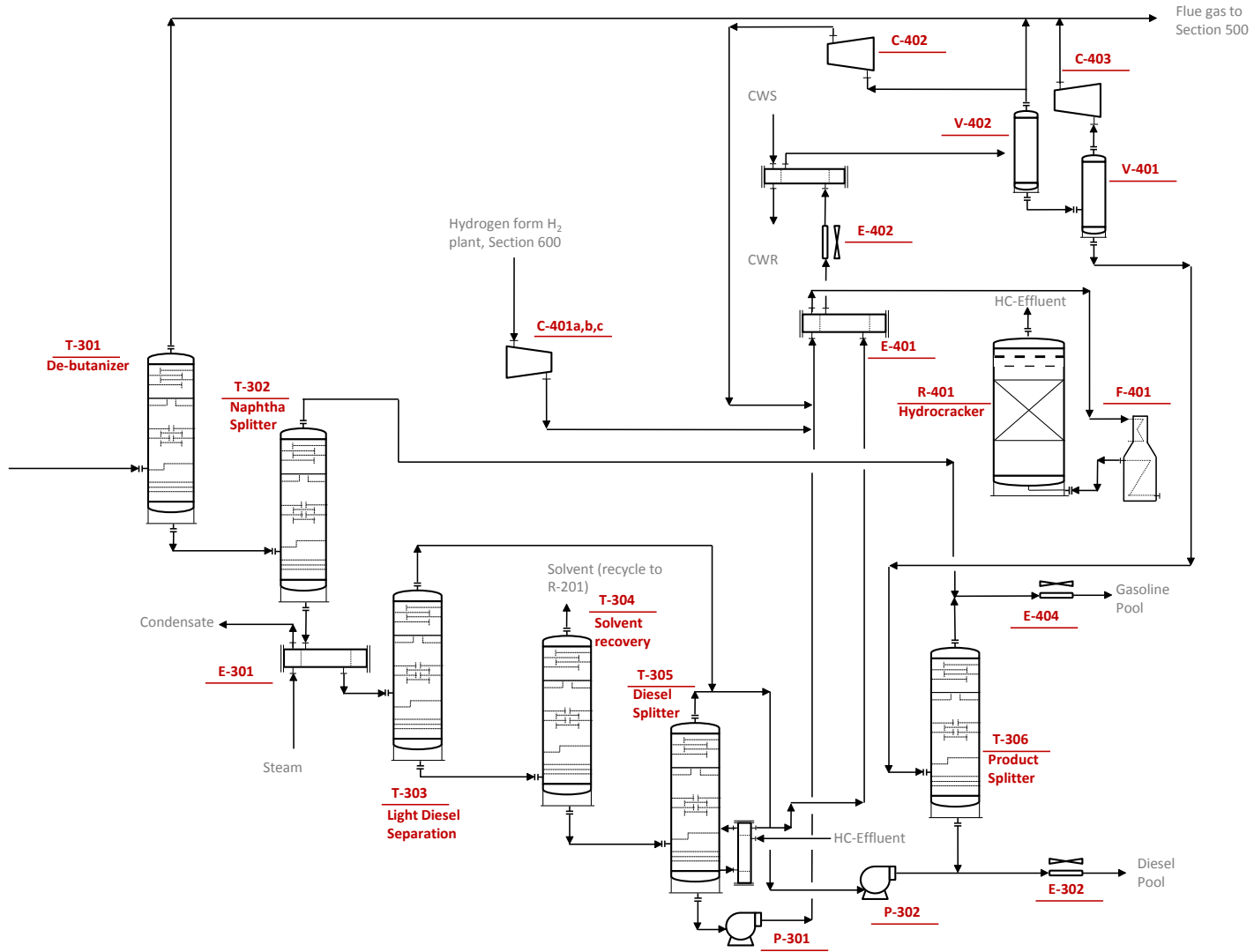


Fig. S4. Separation Section (300) and Hydrocracking Section (400)

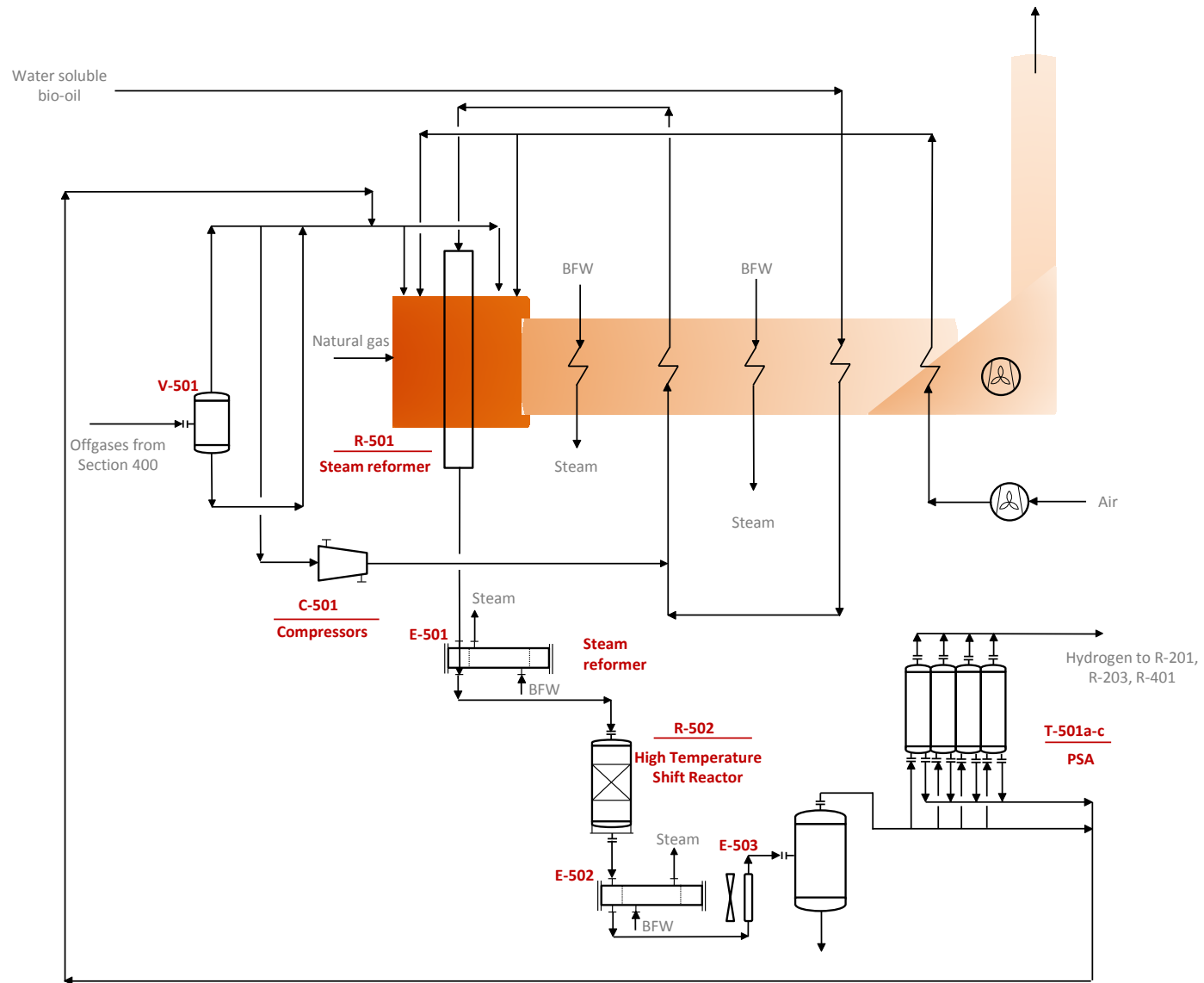


Fig. S5. Hydrogen production Section (500) - adapted from Jones, *et al.*, [51]